A változócsillagászat legújabb eredményeiből

Kiss László akadémikus
MTA CSFK KTM CSI

Polaris Csillagvizsgáló - JD 2457001,25


Megjelent!
meteor
csillagászati évkönyv
2015

Égboltfelmérések, nagy katalógusok

OGLE-II vs. OGLE-III

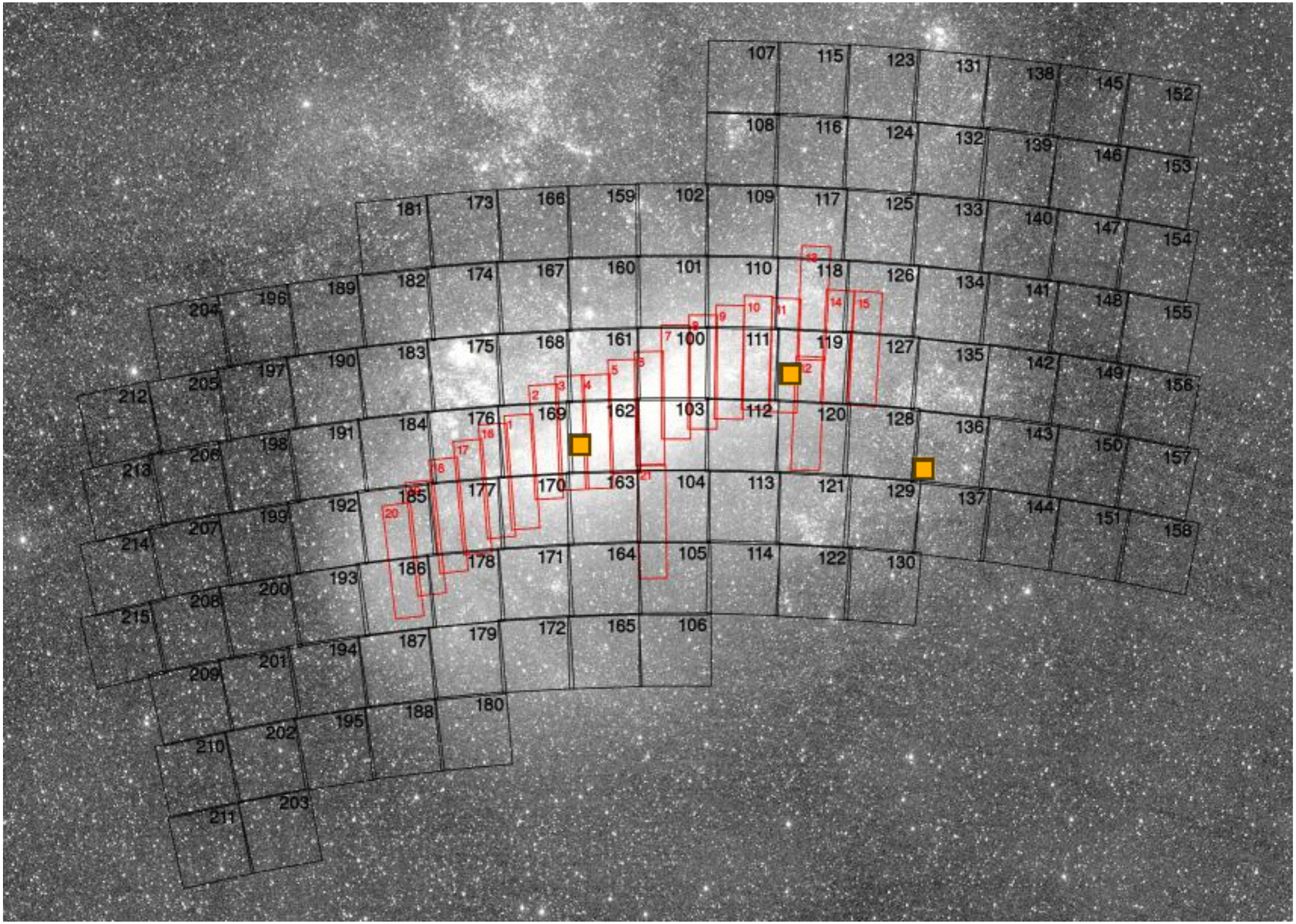

OGLE-IV fields

Galactic coordinates
2013

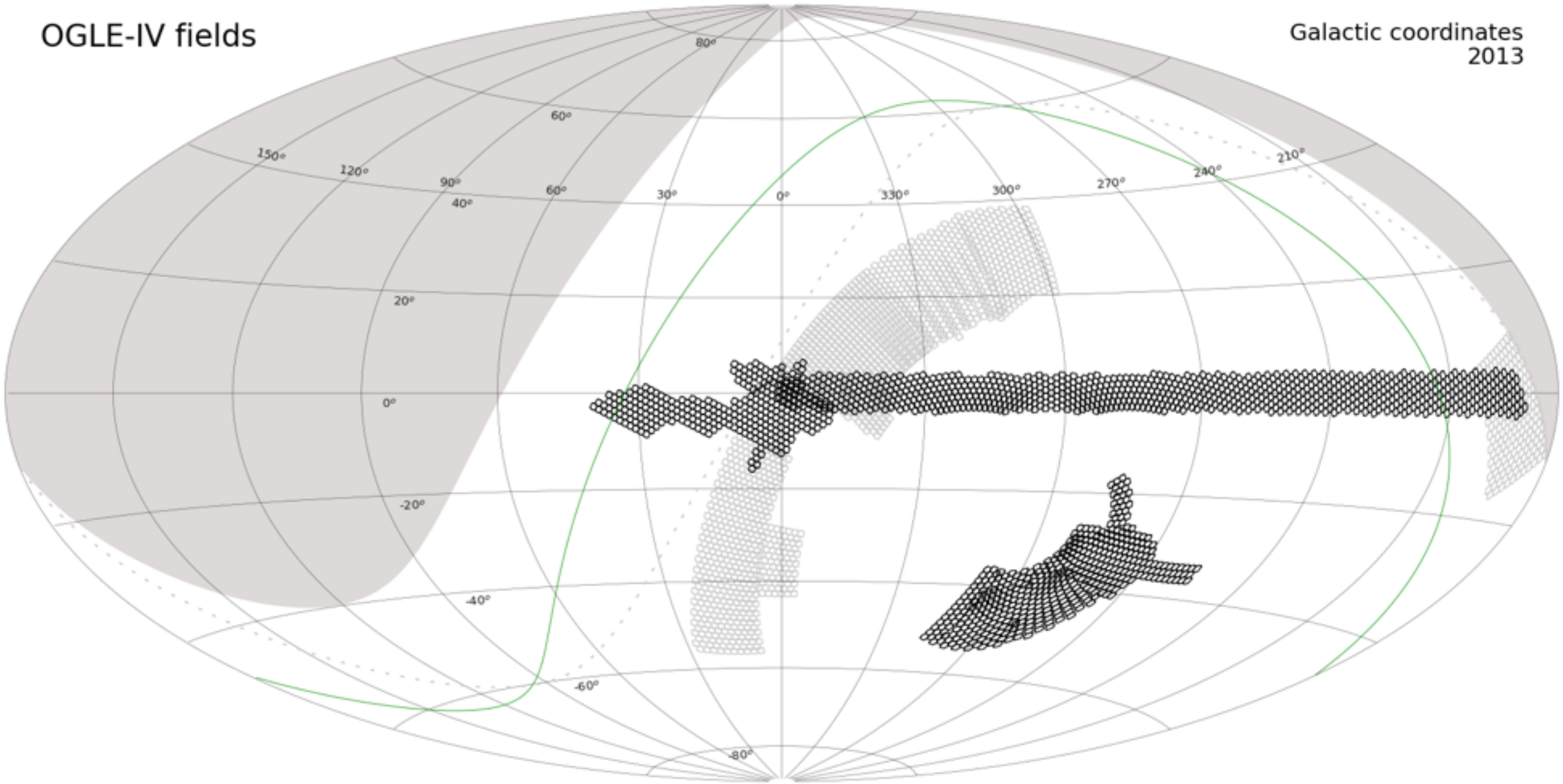

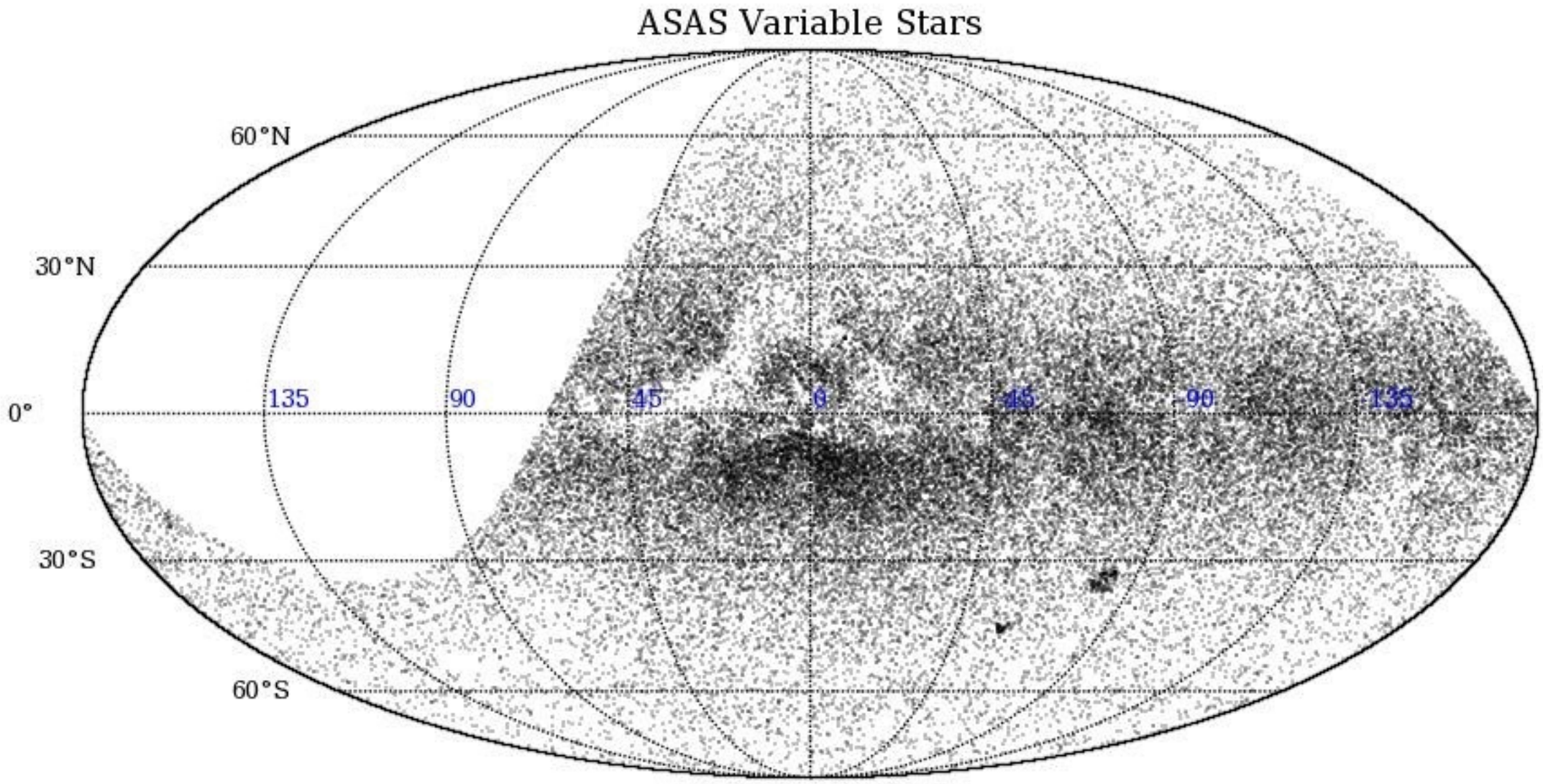
ASAS Variable Stars
60°N
30°N
0°
30°S
60°S
135
90
45
0
45
90
135

V 9.30 [~] C 2002yCat.2237....0D
R 9.2 [~] E 2003yCat.2246....0C
J 9.219 [0.023] C 2003yCat.2246....0C
H 9.202 [0.025] C 2003yCat.2246....0C
K 9.167 [0.021] C 2003yCat.2246....0C

Identifiers (23) :

V* PV Tel
ALS 16142
CD-56 7300
CPC 20 5911
CPD-56 8755
DENIS J182314.6-563744
GCRV 6135 E
GEN# +1.00168476
GSC2 S3123231427
GSC 08752-02335
HD 168476
HIC 90099
HIP 90099
2MASS J18231466-5637441
NSV 10687
PPM 346821
Renson 47210
SAO 245434
TYC 8752-2335-1
UBV 15599
UBV M 22843
uvby98 100168476 V
AAVSO 1814-56

Plots and Images

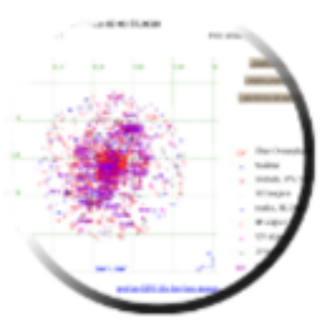

plot

radius 10 arcmin

CDS portal

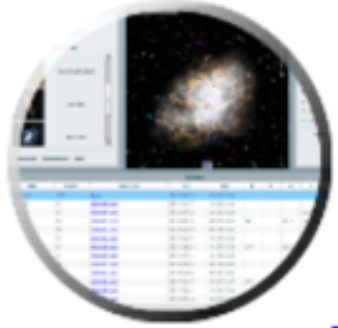

CDS Simplay
(requires flash)

Aladin applet

References (101 between 1850 and 2014)

Simbad bibliographic survey began in 1950 for stars (at least bright stars) and in 1983 for all other objects (outside the solar system).

display
reference summary

from: 1850 to: $currentYear

Változócsillagok és a Tejútrendszer szerkezete

The Astronomical Journal, 146:21 (17pp), 2013 August doi:10.1088/0004-6256/146/2/21

EXPLORING THE VARIABLE SKY WITH LINEAR. II. HALO STRUCTURE AND SUBSTRUCTURE TRACED BY RR LYRAE STARS TO 30 kpc

Branimir Sesar[1], Željko Ivezić[2], J. Scott Stuart[3], Dylan M. Morgan[2], Andrew C. Becker[2], Sanjib Sharma[4], Lovro Palaversa[5], Mario Jurić[6,7], Przemyslaw Wozniak[8], and Hakeem Oluseyi[9]
[1] Division of Physics, Mathematics and Astronomy, Caltech, Pasadena, CA 91125, USA
[2] University of Washington, Department of Astronomy, P.O. Box 351580, Seattle, WA 98195-1580, USA
[3] Lincoln Laboratory, Massachusetts Institute of Technology, 244 Wood Street, Lexington, MA 02420-9108, USA
[4] Sydney Institute for Astronomy, School of Physics, University of Sydney, NSW 2006, Australia
[5] Observatoire astronomique de l'Université de Genève, 51 chemin des Maillettes, CH-1290 Sauverny, Switzerland
[6] Steward Observatory, University of Arizona, Tucson, AZ 85121, USA
[7] LSST Corporation, 933 North Cherry Avenue, Tucson, AZ 85721, USA
[8] Los Alamos National Laboratory, 30 Bikini Atoll Rd., Los Alamos, NM 87545-0001, USA
[9] Florida Institute of Technology, Melbourne, FL 32901, USA
Received 2013 February 3; accepted 2013 May 8; published 2013 June 27

We present a sample of ~5000 RR Lyrae stars selected from the recalibrated LINEAR data set and detected at heliocentric distances between 5 kpc and 30 kpc over ~8000 deg^2 of sky. The coordinates and light curve properties, such as period and Oosterhoff type, are made publicly available. We analyze in detail the light curve properties and Galactic distribution of the subset of ~4000 type ab RR Lyrae (RRab) stars, including a search for new halo substructures and the number density distribution as a function of Oosterhoff type. We find evidence for the Oosterhoff dichotomy among field RR Lyrae stars, with the ratio of the type II and I subsamples of about 1:4, but with a weaker separation than for globular cluster stars. The wide sky coverage and depth of this sample allow unique constraints for the number density distribution of halo RRab stars as a function of galactocentric distance: it can be described as an oblate ellipsoid with an axis ratio $q = 0.63$ and with either a single or a double power law with a power-law index in the range -2 to -3. Consistent with previous studies, we find that the Oosterhoff type II subsample has a steeper number density profile than the Oosterhoff type I subsample. Using the group-finding algorithm EnLink, we detected seven candidate halo groups, only one of which is statistically spurious. Three of these groups are near globular clusters (M53/NGC 5053, M3, M13), and one is near a known halo substructure (Virgo Stellar Stream); the remaining three groups do not seem to be near any known halo substructures or globular clusters and seem to have a higher ratio of Oosterhoff type II to Oosterhoff type I RRab stars than what is found in the halo. The extended morphology and the position (outside the tidal radius) of some of the groups near globular clusters are suggestive of tidal streams possibly originating from globular clusters. Spectroscopic follow-up of detected halo groups is encouraged.

Key words: Galaxy: halo – Galaxy: stellar content – Galaxy: structure – stars: variables: RR Lyrae

Online-only material: animation, color figures, machine-readable and VO tables, supplemental data (FITS)

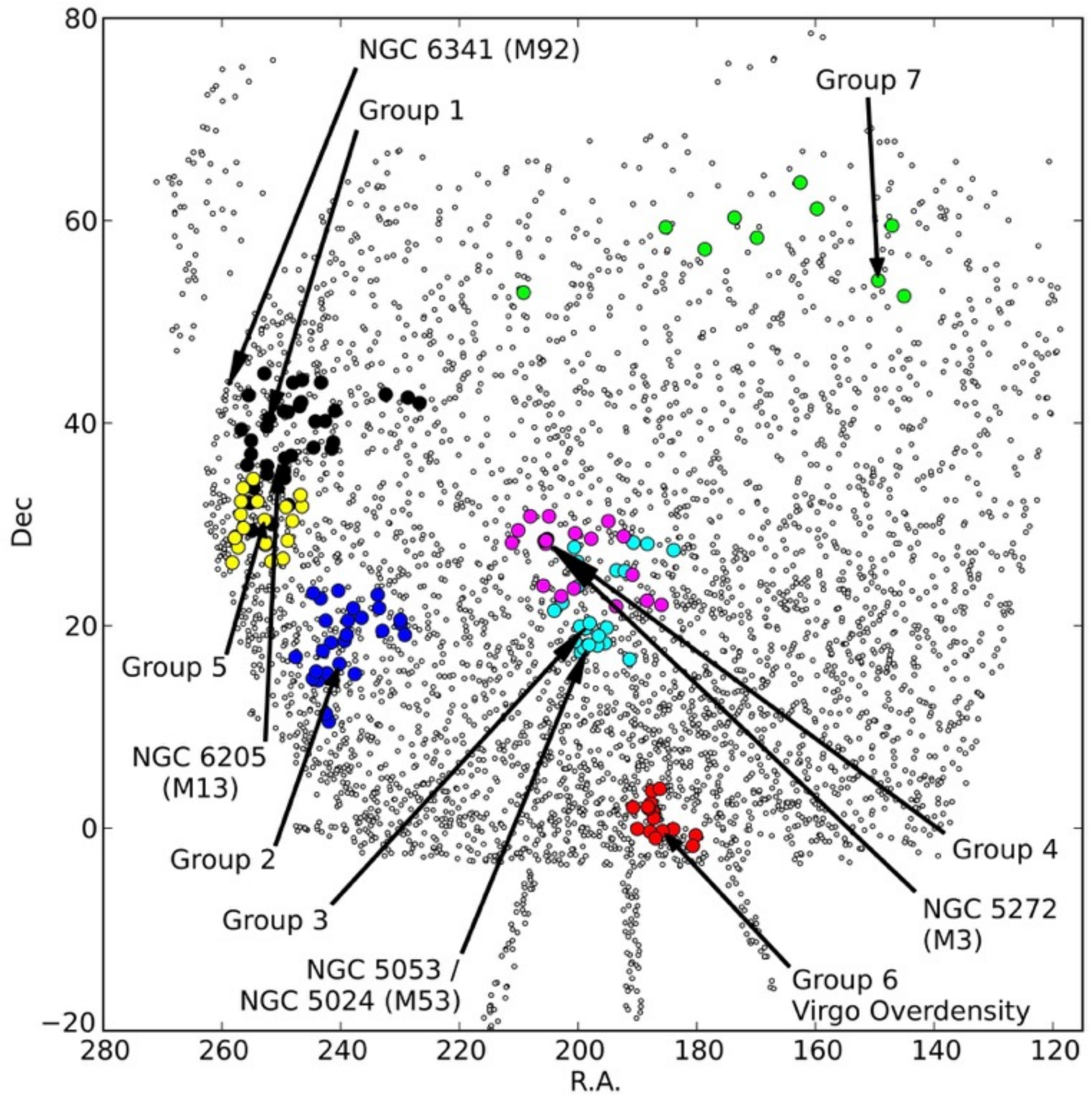
NGC 6341 (M92)
Group 1
Group 7
Group 5
NGC 6205
(M13)
Group 2
Group 3
NGC 5053 /
NGC 5024 (M53)
Group 4
NGC 5272
(M3)
Group 6
Virgo Overdensity
80
60
40
20
0
−20
Dec
280
260
240
220
200
180
160
140
120
R.A.

Group 1

Group 2

Group 3 (M53/NGC 5053)

Group 4 (M3)

Group 5 (M13)

Group 6 (Virgo)

Group 7

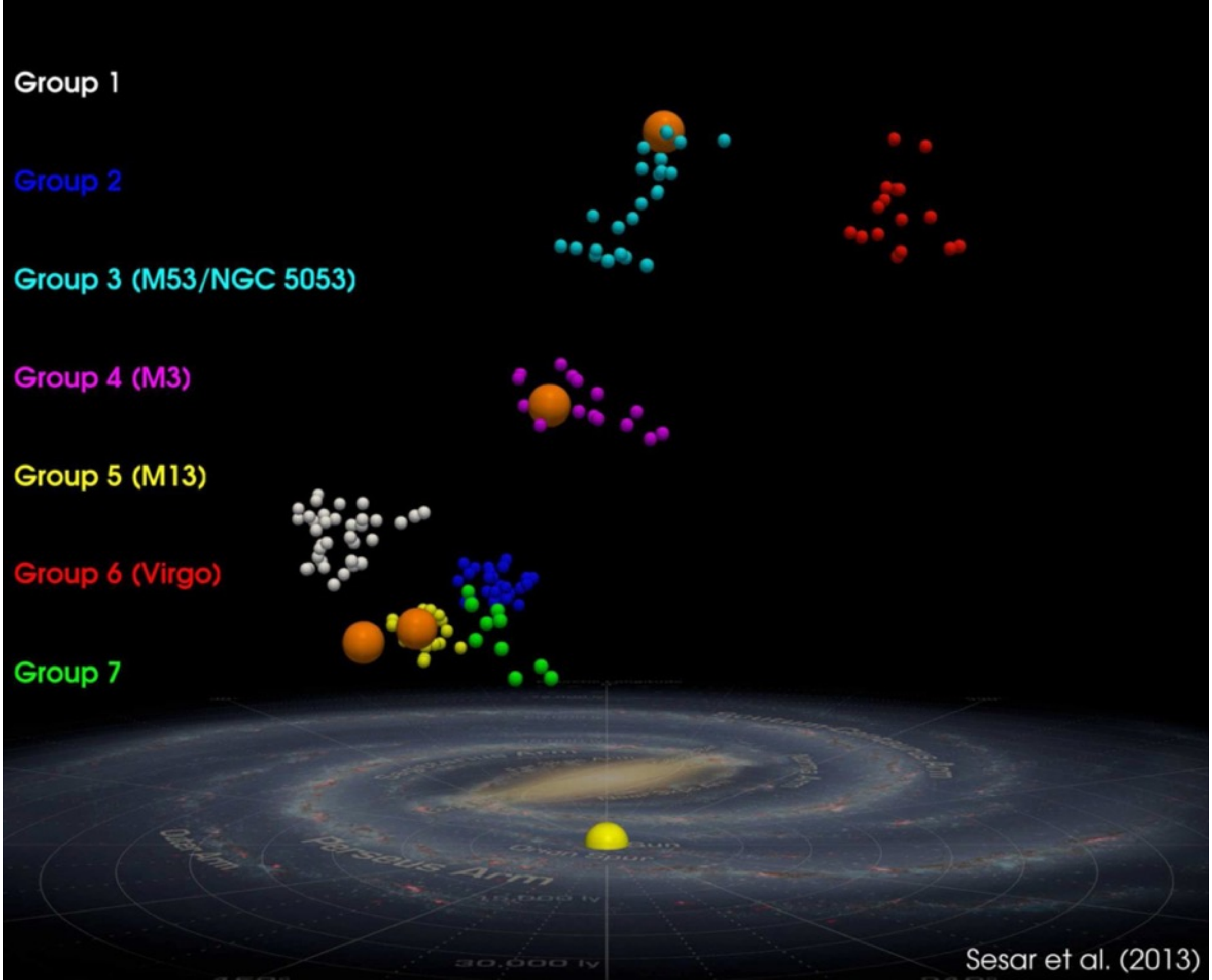

Sesar et al. (2013)

Kataklizmikus változók és a nagy minták módszere

Cataclysmic variables from the Catalina Real-time Transient Survey

A. J. Drake,[1]★ B. T. Gänsicke,[2] S. G. Djorgovski,[1] P. Wils,[3] A. A. Mahabal,[1] M. J. Graham,[1] T.-C. Yang,[1,4] R. Williams,[1] M. Catelan,[5,6] J. L. Prieto,[7] C. Donalek,[1] S. Larson[8] and E. Christensen[8]

[1] *California Institute of Technology, 1200 E. California Blvd, CA 91225, USA*
[2] *Department of Physics, University of Warwick, Coventry CV4 7AL, UK*
[3] *Vereniging voor Sterrenkunde, Belgium*
[4] *National Central University, JhongLi City, Taiwan*
[5] *Pontificia Universidad Católica de Chile, Insituto de Astrofísica, 782-0436 Macul, Santiago, Chile*
[6] *The Milky Way Millennium Nucleus, Santiago, Chile*
[7] *Department of Astronomy, Princeton University, 4 Ivy Ln, Princeton, NJ 08544, USA*
[8] *Department of Planetary Sciences, The University of Arizona, 1629 E. University Blvd, Tucson, AZ 85721, USA*

Accepted 2014 April 1. Received 2014 March 31; in original form 2013 April 5

ABSTRACT

We present 855 cataclysmic variable candidates detected by the Catalina Real-time Transient Survey (CRTS) of which at least 137 have been spectroscopically confirmed and 705 are new discoveries. The sources were identified from the analysis of five years of data, and come from an area covering three quarters of the sky. We study the amplitude distribution of the dwarf novae cataclysmic variables (CVs) discovered by CRTS during outburst, and find that in quiescence they are typically 2 mag fainter compared to the spectroscopic CV sample identified by the Sloan Digital Sky Survey. However, almost all CRTS CVs in the SDSS footprint have *ugriz* photometry. We analyse the spatial distribution of the CVs and find evidence that many

2 OBSERVATIONAL DATA

The Catalina Sky Survey[1] began in 2004 and uses three telescopes to repeatedly survey the sky between declination $\delta = -75$ and $+65^\circ$ in search of Near-Earth Objects (NEOs) and Potential Hazardous Asteroids (PHAs). In addition to asteroids, all the Catalina data are analysed for transient sources by CRTS (Drake et al. 2009a; Djorgovski et al 2011).

Each of the survey telescopes is run as separate sub-surveys. These consist of the Catalina Schmidt Survey (CSS), the Mount Lemmon Survey (MLS) and the Siding Spring Survey (SSS). In this paper we analyse data taken by all three telescopes, namely the 0.7-m CSS telescope and the 1.5-m MLS telescope in Tucson, AZ, and the 0.5m (SSS) Uppsala Schmidt at Siding Spring Observatory, Australia. Transient processing of CSS data by CRTS began on 2007 November 8, while for MLS data it began on 2009 November 6, and for SSS on 2010 May 5.

Each telescope currently has a 4k $\times$ 4k CCD camera, which for the CSS, MLS and SSS cover 8.2, 1.1 and 4 $\deg^2$, respectively. In general each telescope avoids the Galactic latitudes less than 10 to 15° due to reduced source recovery in crowded stellar regions. Because of its smaller field-of-view the MLS 1.5-m telescope predominately observes only ecliptic latitudes $-10^\circ < \beta < 10^\circ$,

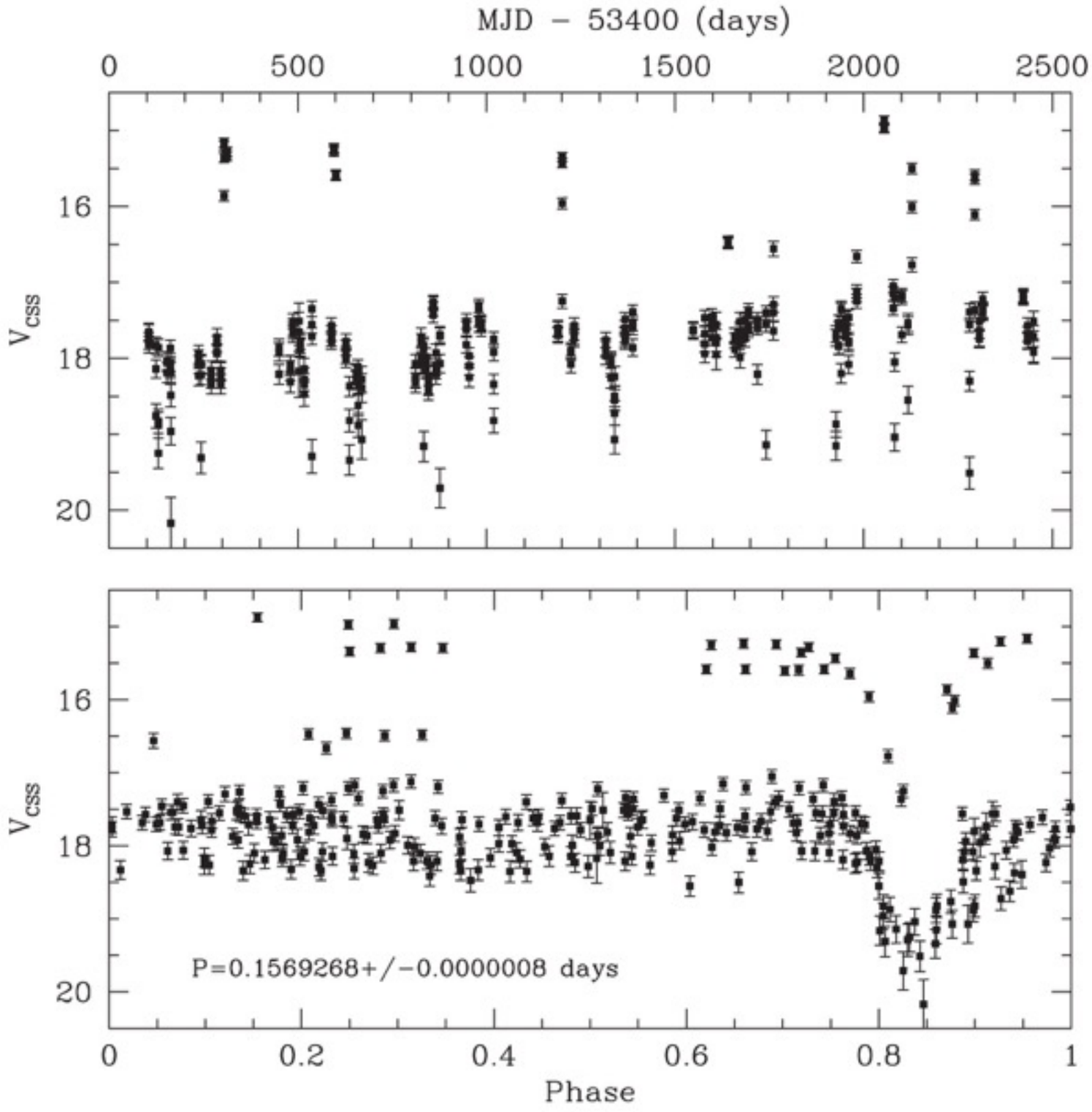
MJD − 53400 (days)
0
500
1000
1500
2000
2500
16
18
20
V_{CSS}
P=0.1569268+/−0.0000008 days
0
0.2
0.4
0.6
0.8
1
Phase

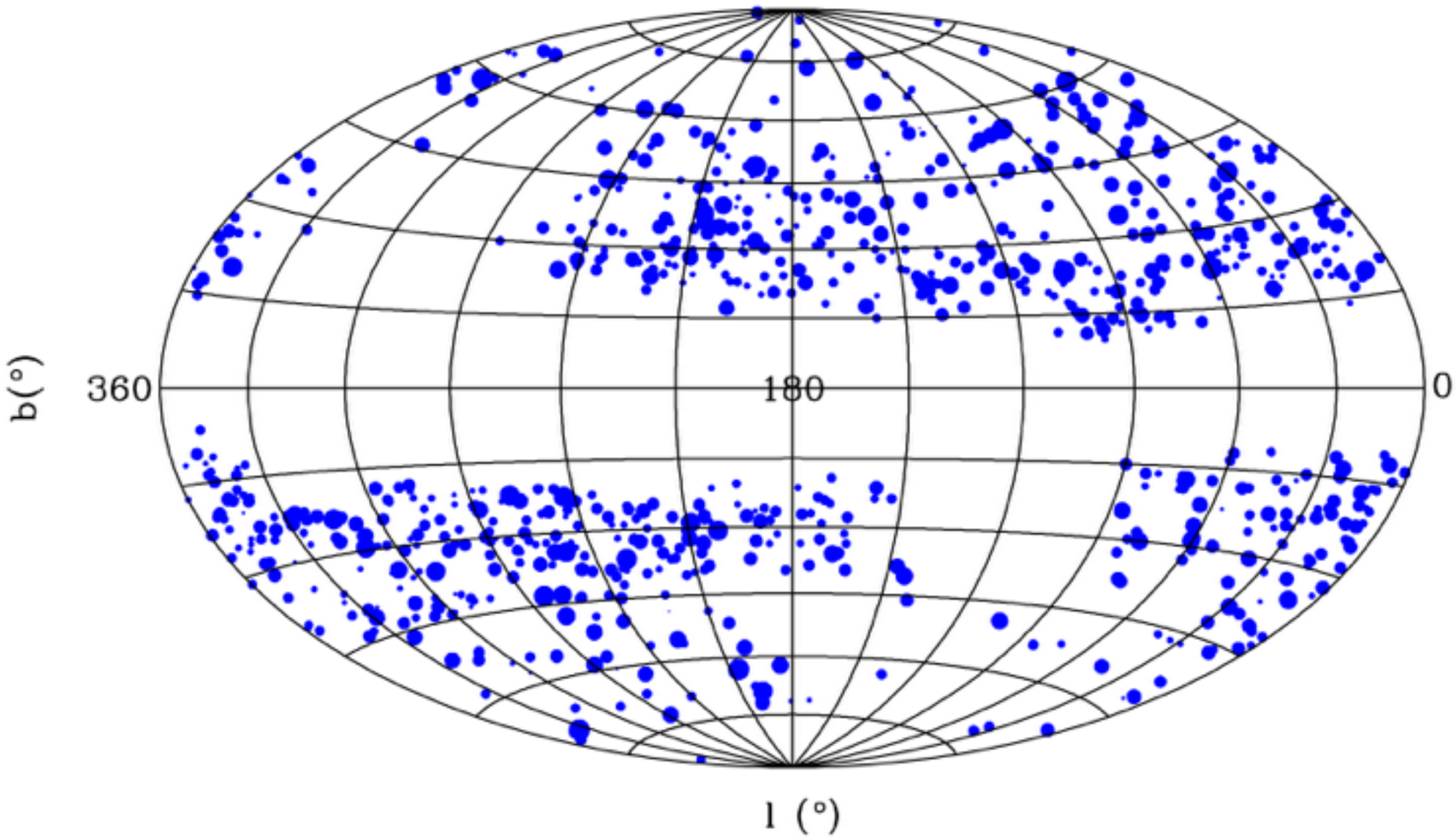

Figure 1. The distribution of CRTS CV candidates in Galactic coordinates (Aitoff projection). The radii of the points are proportional to the peak magnitude with the brightest points largest. Gaps are present in the regions not observed by Catalina, i.e. near the celestial poles and in the galactic plane.

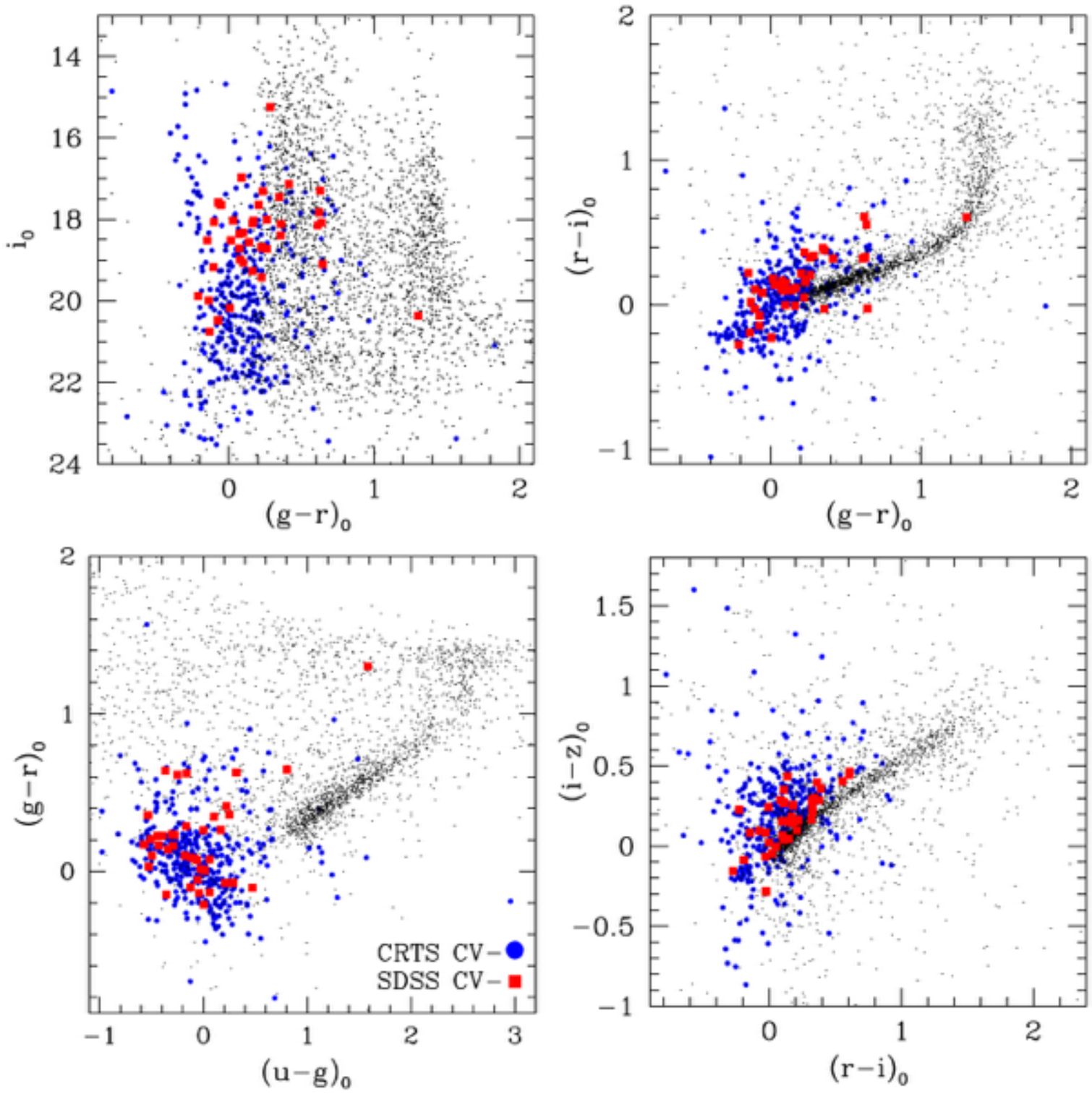

Figure 5. The colour and brightness distribution of CRTS CV candidates. CV candidates are large blue dots. Red squares are sources with SDSS spectra. The black points are the point sources (stars, QSOs and other unresolved sources) from the SDSS that lie within an arcmin of each CV candidate.

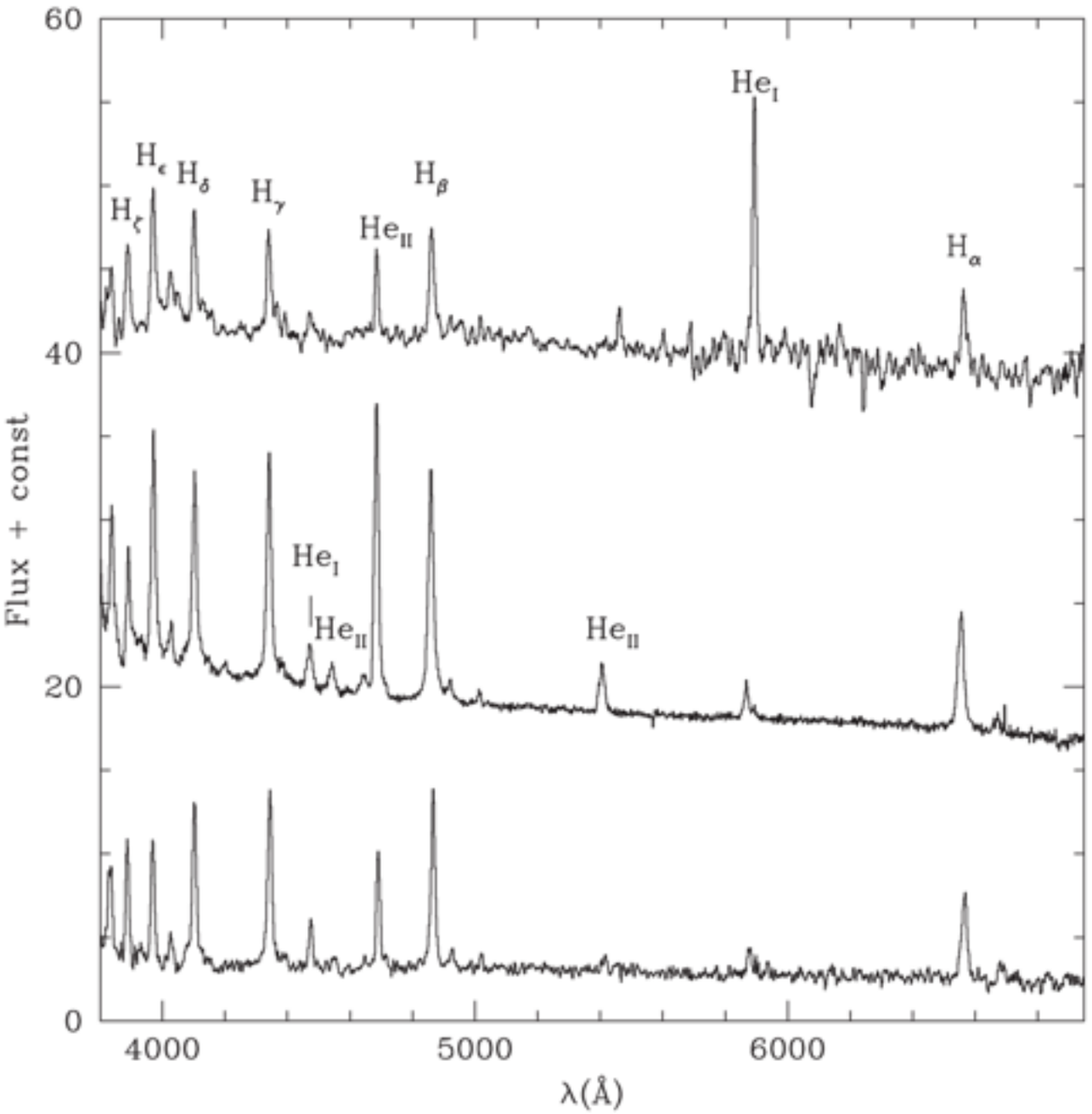

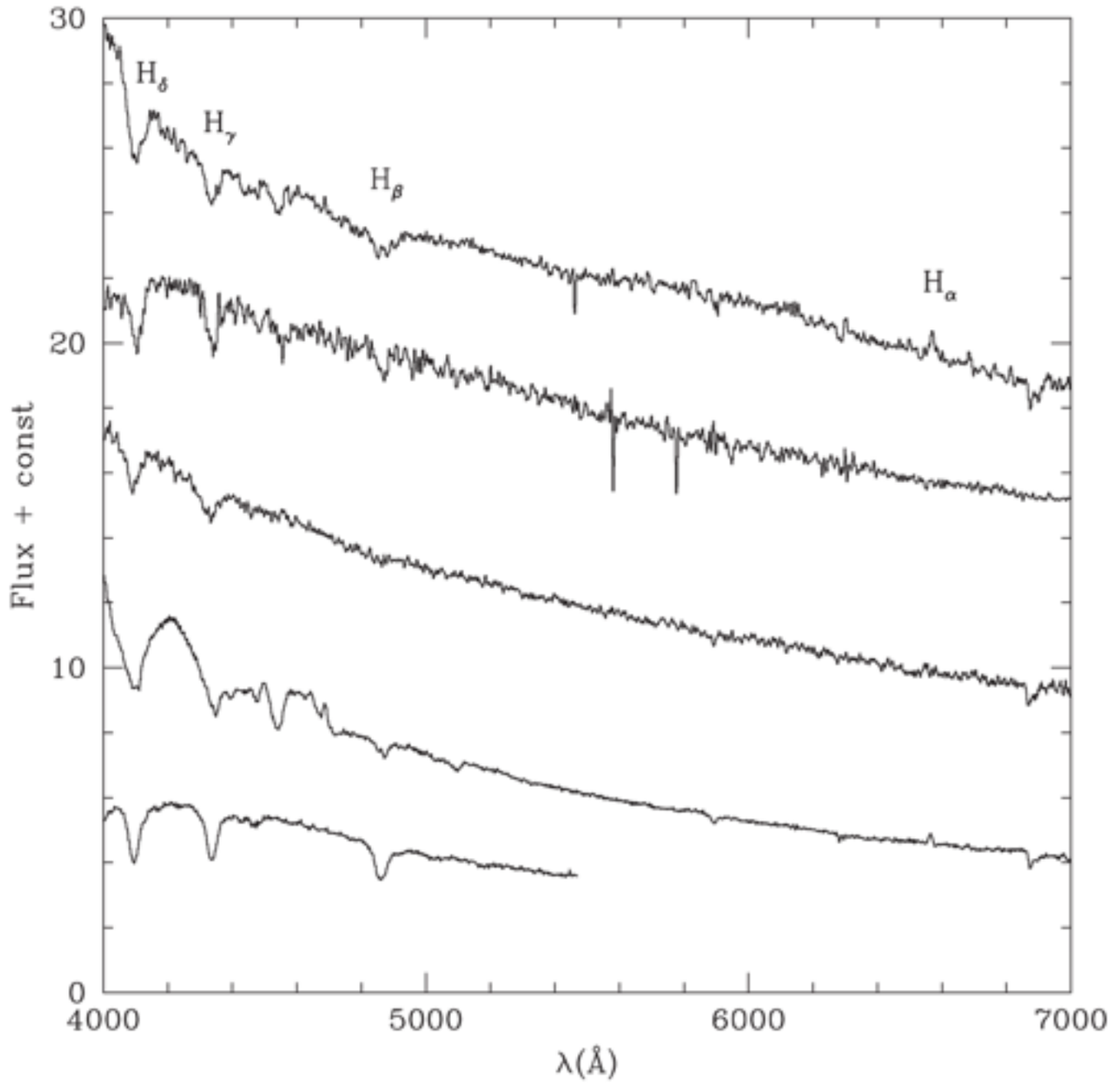

Figure 11. Palomar 5-m spectra of CRTS CVs. In the left panel (top to bottom), we show spectra of three CVs (CSS100108:081031+002429, CSS110114:091937−055519, CSS100313:085607+123837) exhibiting strong hydrogen and helium emission lines typical of CVs near quiescence. In the right panel (top to bottom), we show the spectra of CRTS CVs that were observed during outburst (CSS120113:040822+141516, CSS100507:164354−131525, CSS110623:173517+154708, CSS080606:162322+121334, CSS110501:094825+204333).

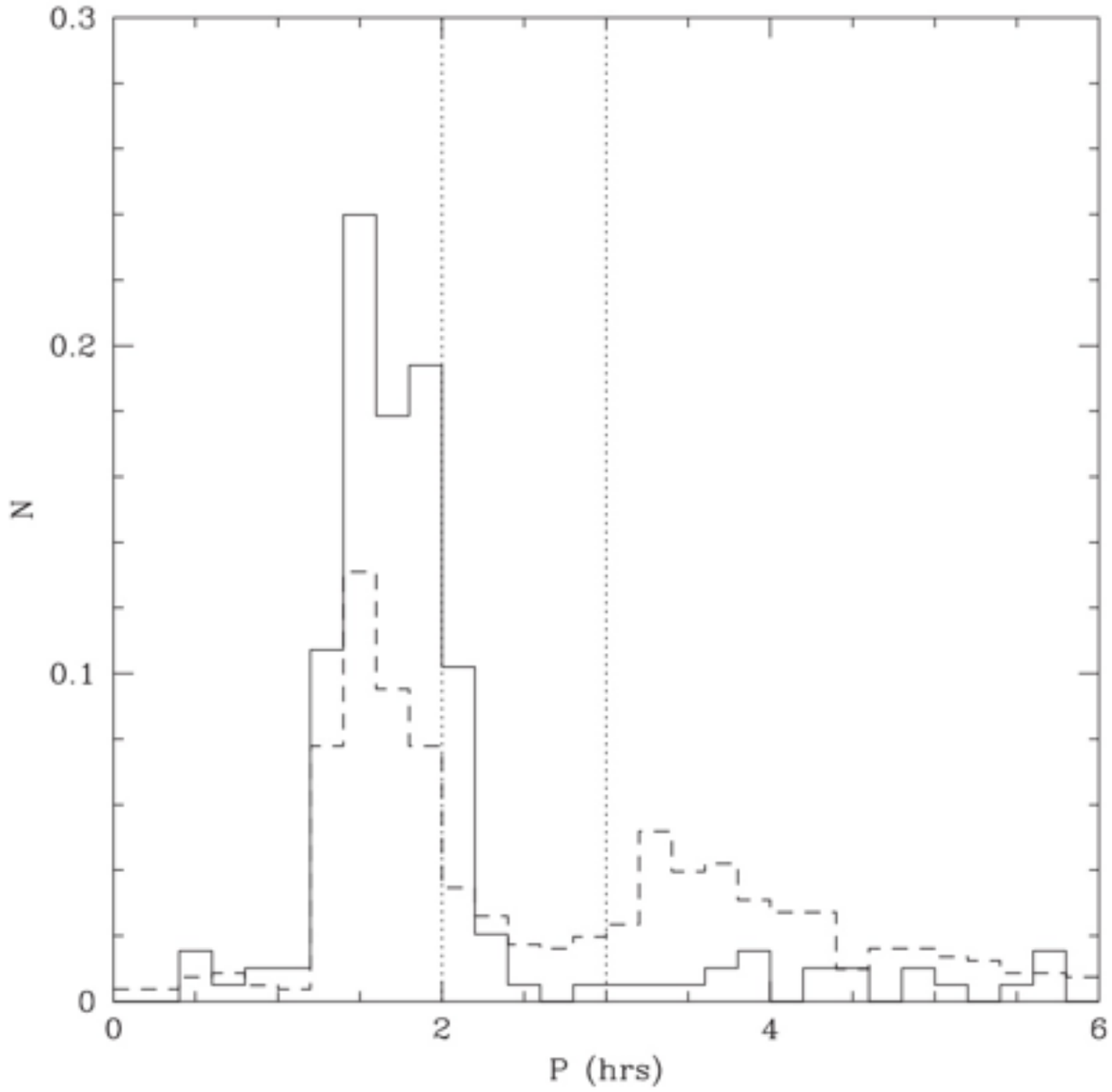

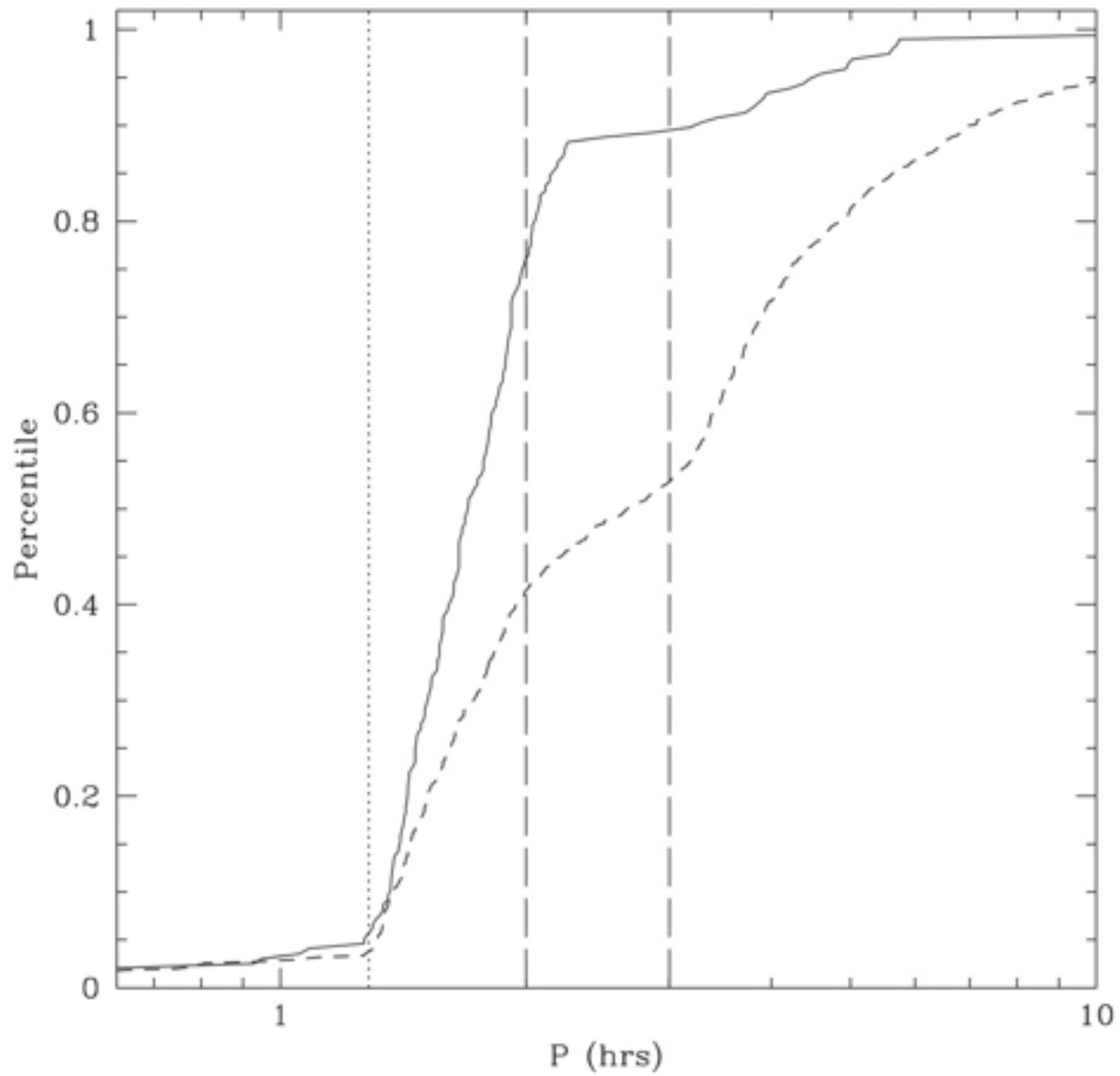

Figure 16. The normalized CV period distribution. On the left panel, we plot the distribution of CV periods for sources detected by CRTS (solid line) and the distribution of all CV periods given by Ritter & Kolb (2003, dashed line). On the right panel, we plot the cumulative distribution of CV periods. In the right panel CV, the period-minimum is plotted with a dotted line, while the period gap is indicated by the region between the two long-dashed lines.

Csillagaktivitás és kormeghatározás

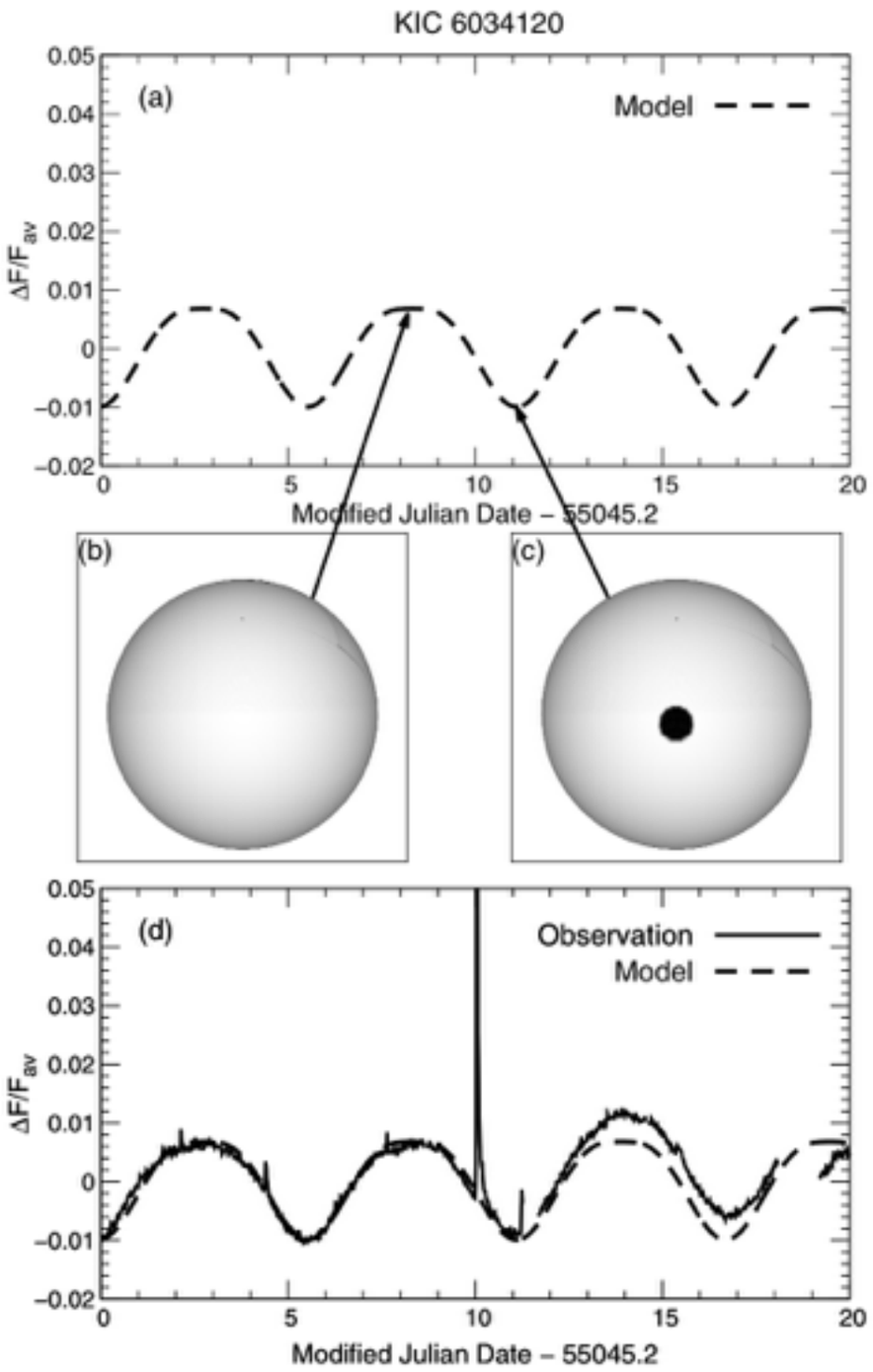

Figure 3. (a) Model light curve for KIC 6034120 (Figure 1(a)). The model parameters are given in Table 3. (b) and (c) Model images of the visible area of the photosphere with a starspot. (d) Observed light curve (solid line; the same as in Figure 1(a)) and model light curve (dashed line) for KIC 6034120.

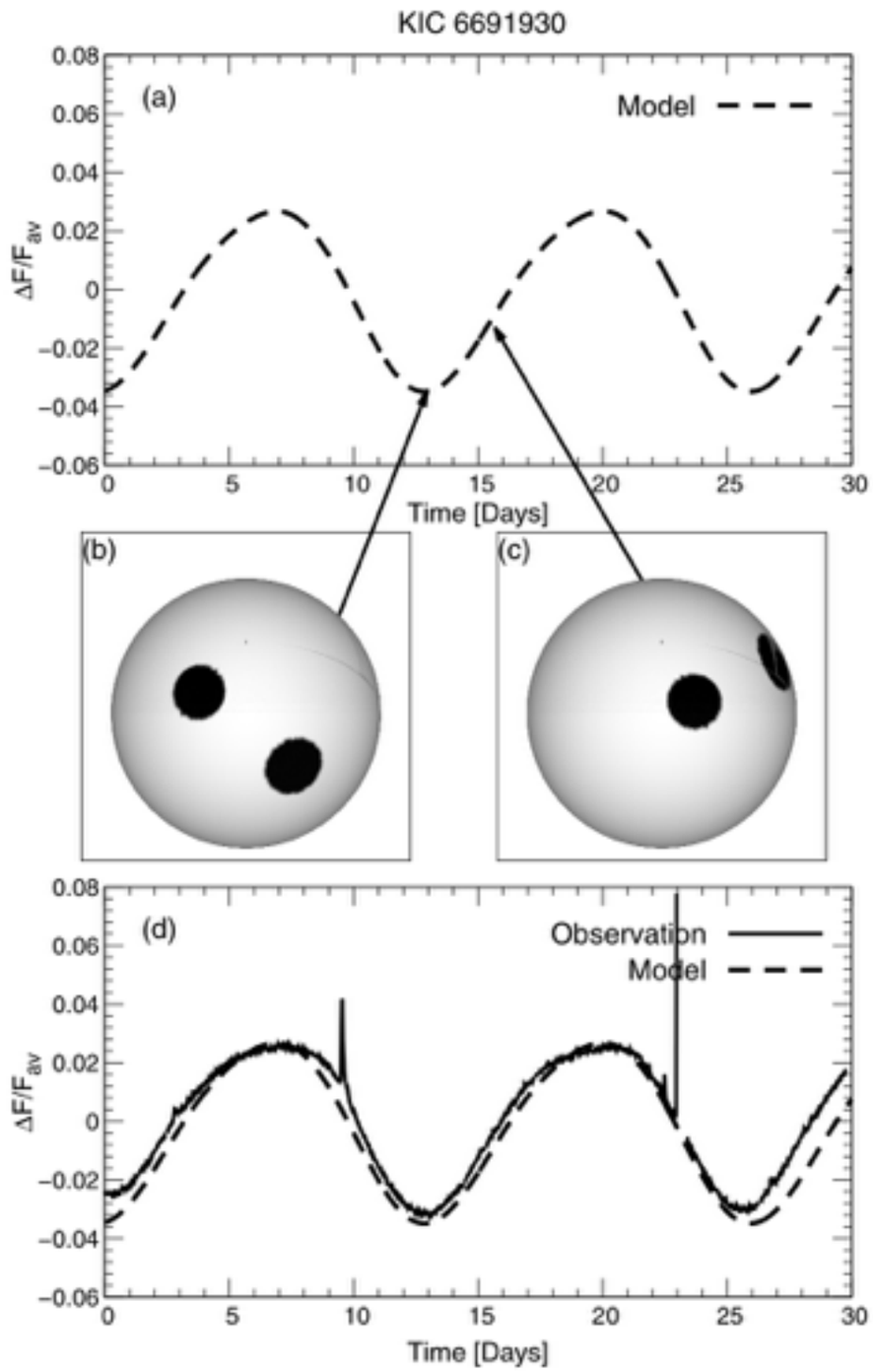

Figure 4. (a) Model light curve for KIC 6691930. The model parameters are given in Table 3. (b) and (c) Model images of the visible area of the photosphere with two starspots. (d) Observed light curve (solid line; the same as in Figure 1(b)) and model light curve (dashed line) for KIC 6691930.

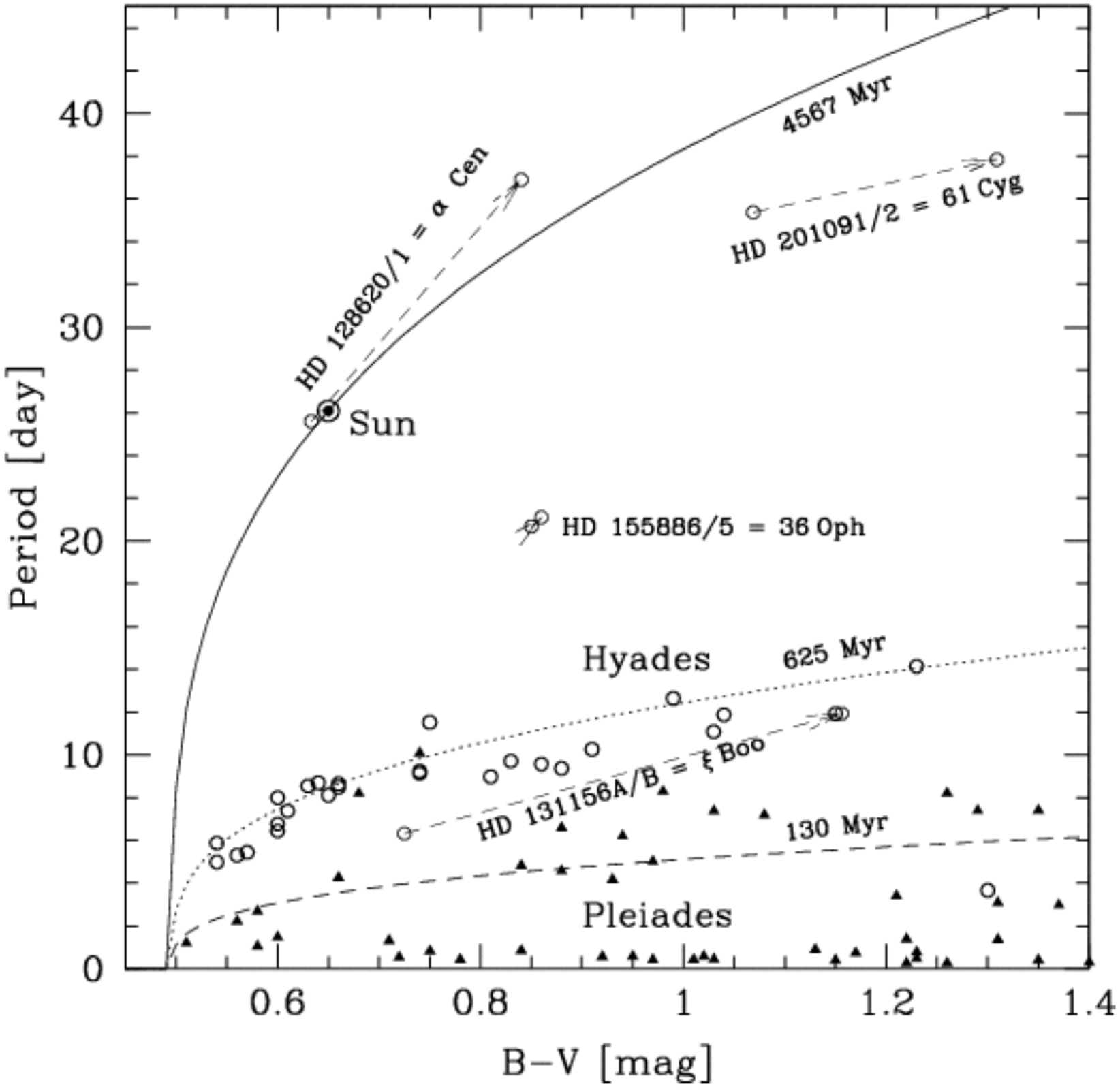
4567 Myr
HD 128620/1 = α Cen
HD 201091/2 = 61 Cyg
Sun
HD 155886/5 = 36 Oph
Hyades
625 Myr
HD 131156A/B = ξ Boo
130 Myr
Pleiades
40
30
20
10
0
0.6
0.8
1
1.2
1.4
B−V [mag]
Period [day]

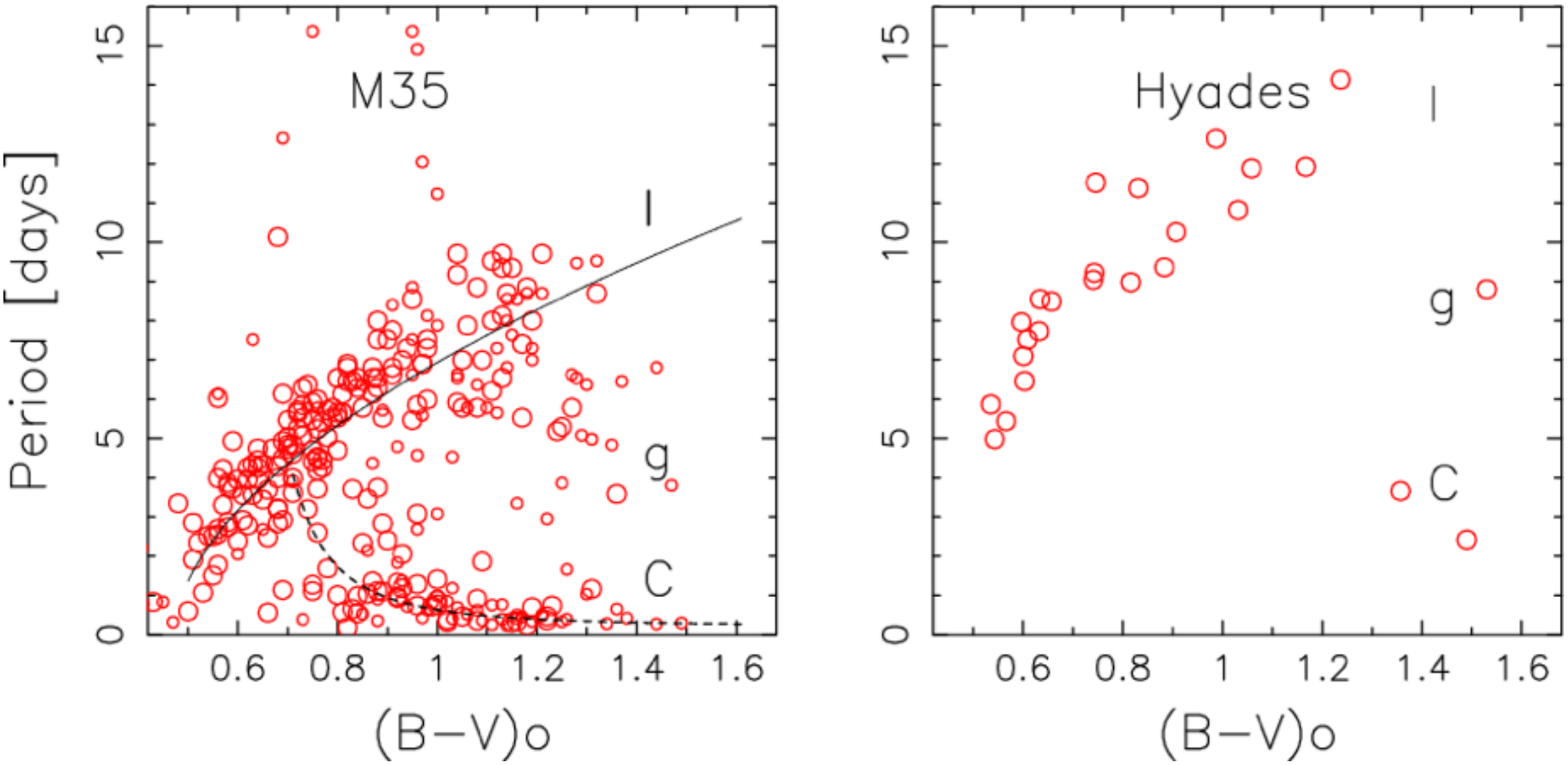
M35
I
g
C
Period [days]
(B−V)o
0
5
10
15
0.6
0.8
1
1.2
1.4
1.6
Hyades
I
g
C
(B−V)o

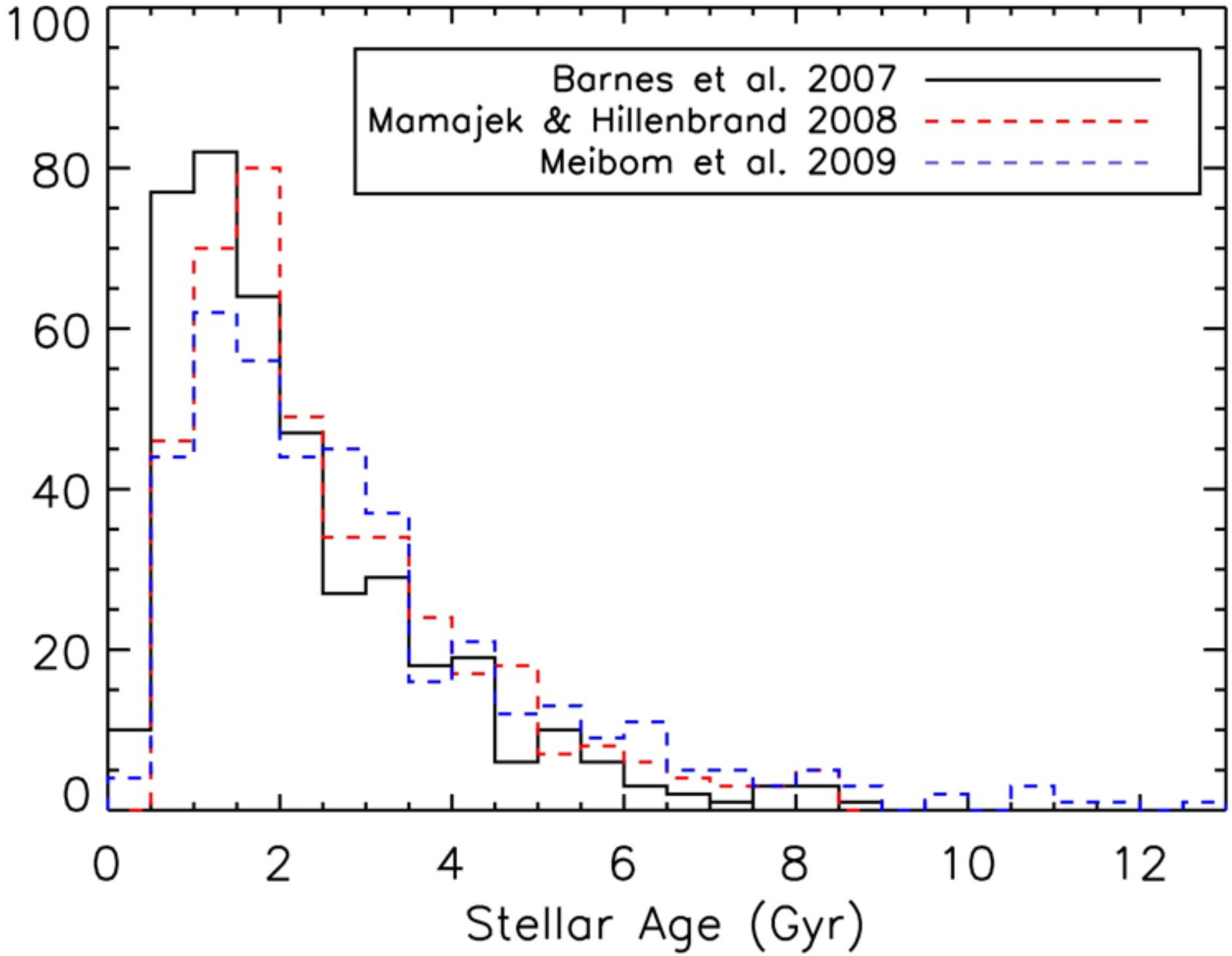
Barnes et al. 2007
Mamajek & Hillenbrand 2008
Meibom et al. 2009
100
80
60
40
20
0
0
2
4
6
8
10
12
Stellar Age (Gyr)

Stellar Rotation [Days]

$R_p \leqq 1.25R_e$

$1.25R_e < R_p \leqq 2R_e$

$2R_e < R_p \leqq 6R_e$

$R_p > 6R_e$

100
10
1
0.1
1.0
10.0
100.0
1000.0

Orbital Period [Days]

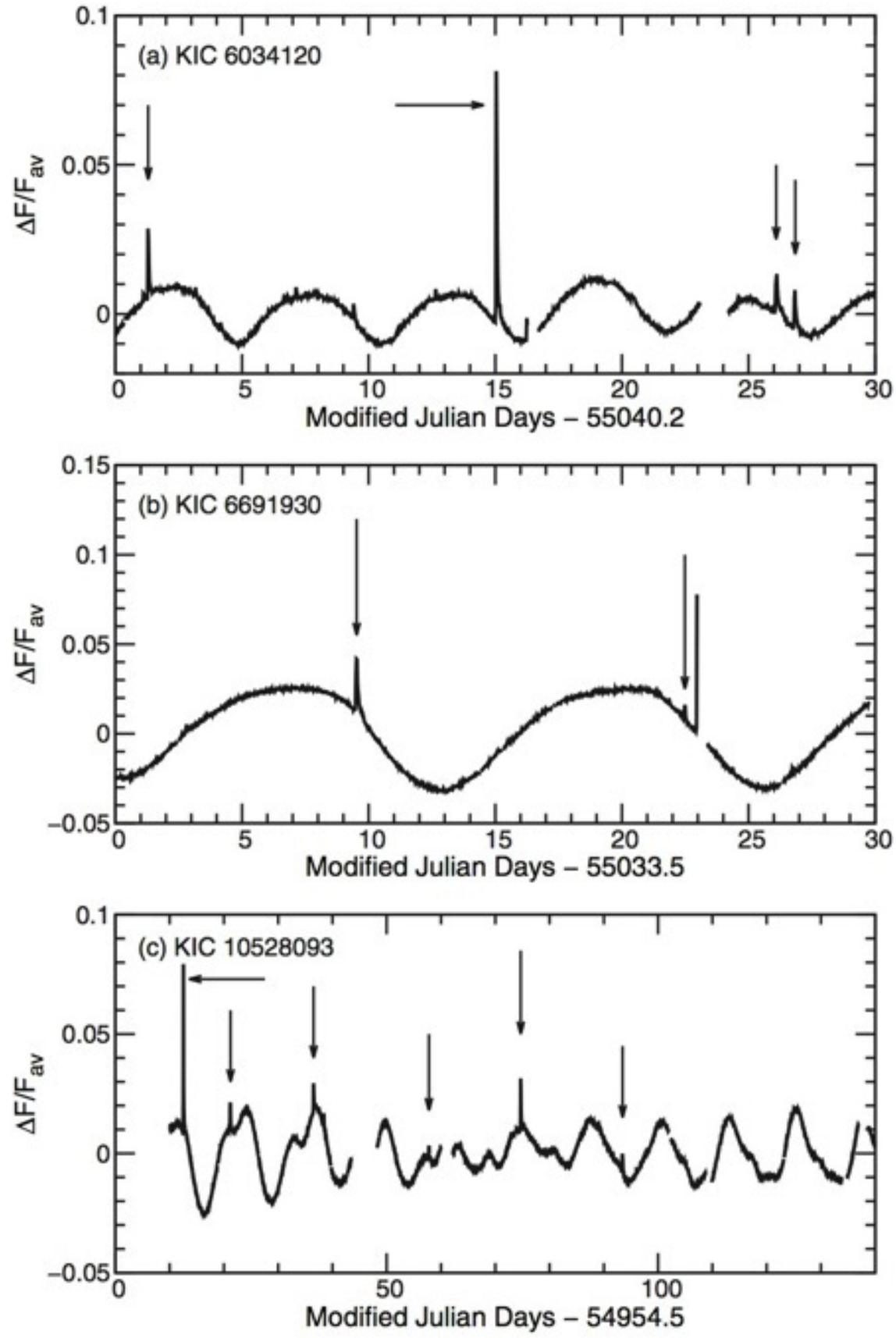
(a) KIC 6034120
0.1
0.05
0
ΔF/F_av
0
5
10
15
20
25
30
Modified Julian Days – 55040.2
(b) KIC 6691930
0.15
0.1
0.05
0
−0.05
ΔF/F_av
0
5
10
15
20
25
30
Modified Julian Days – 55033.5
(c) KIC 10528093
0.1
0.05
0
−0.05
ΔF/F_av
0
50
100
Modified Julian Days – 54954.5

Összeolvadó kettőscsillagok

V838 Mon

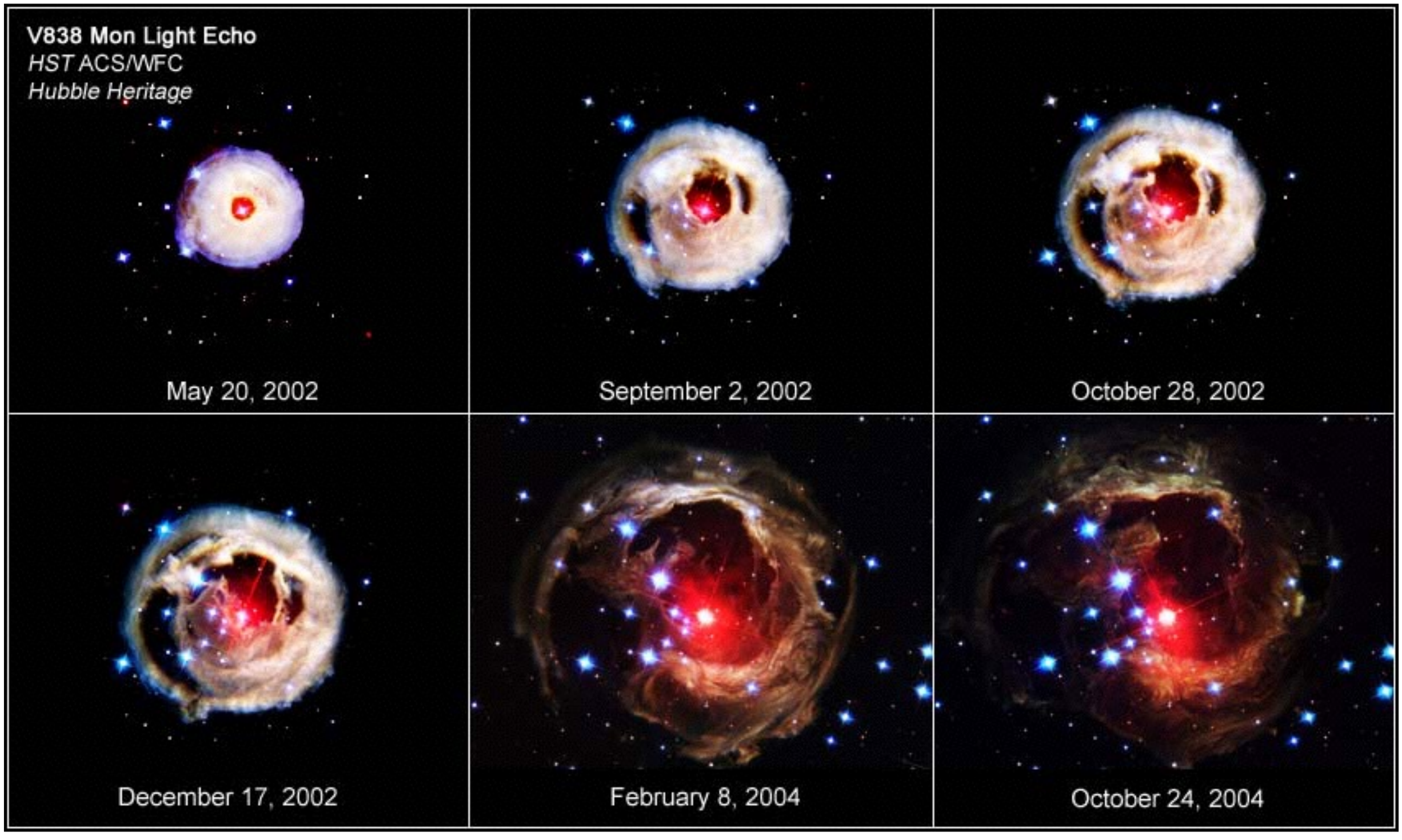
V838 Mon Light Echo
HST ACS/WFC
Hubble Heritage
May 20, 2002
September 2, 2002
October 28, 2002
December 17, 2002
February 8, 2004
October 24, 2004

V1309 Sco

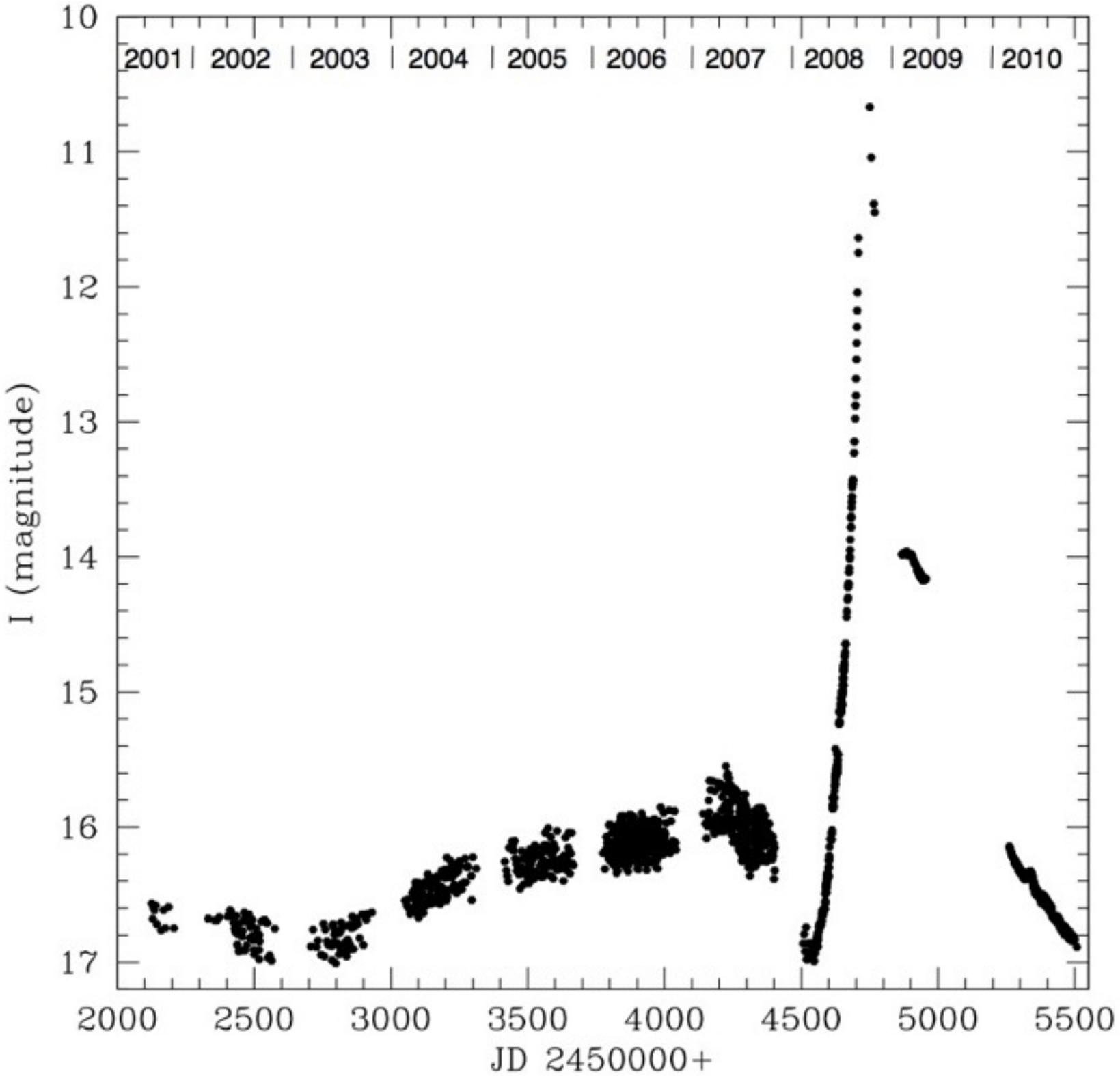
2001
2002
2003
2004
2005
2006
2007
2008
2009
2010
10
11
12
13
14
15
16
17
I (magnitude)
2000
2500
3000
3500
4000
4500
5000
5500
JD 2450000+

V1309 Sco

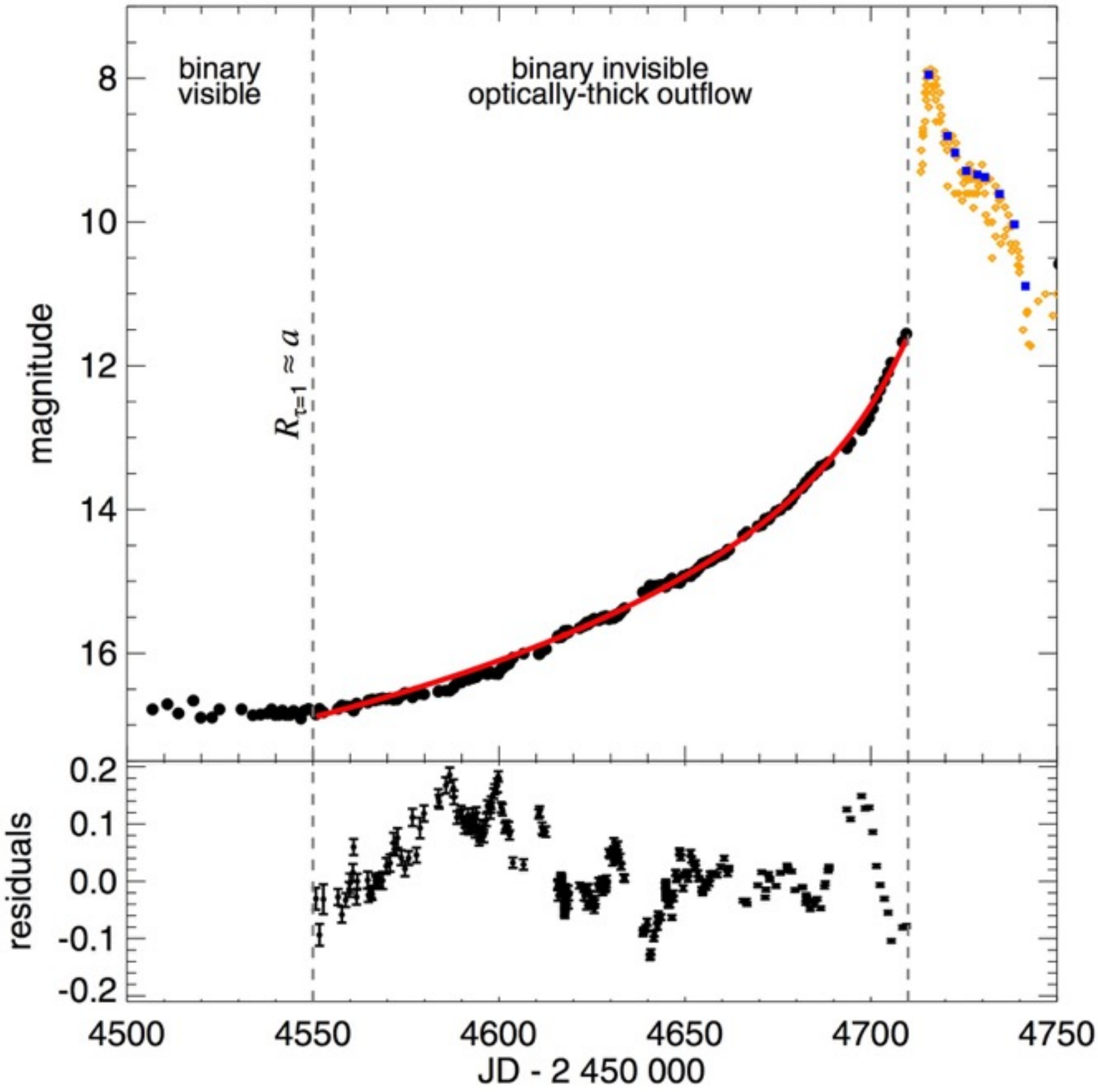
binary
visible
binary invisible
optically-thick outflow
$R_{\tau=1} \approx a$
magnitude
8
10
12
14
16
0.2
0.1
0.0
-0.1
-0.2
residuals
4500
4550
4600
4650
4700
4750
JD - 2 450 000

V1309 Sco

THE ASTROPHYSICAL JOURNAL, 788:22 (7pp), 2014 June 10

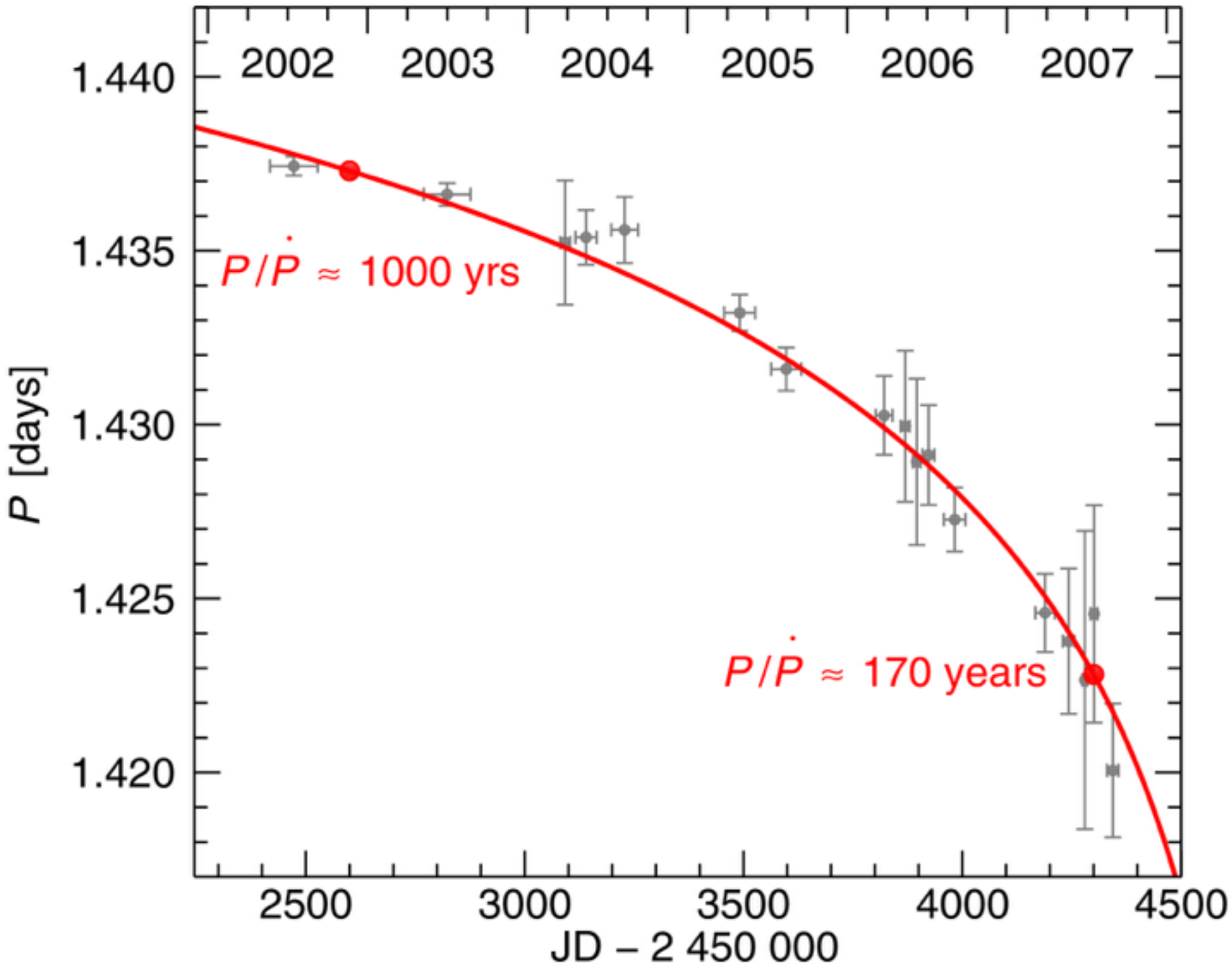

V1309 Sco - modell

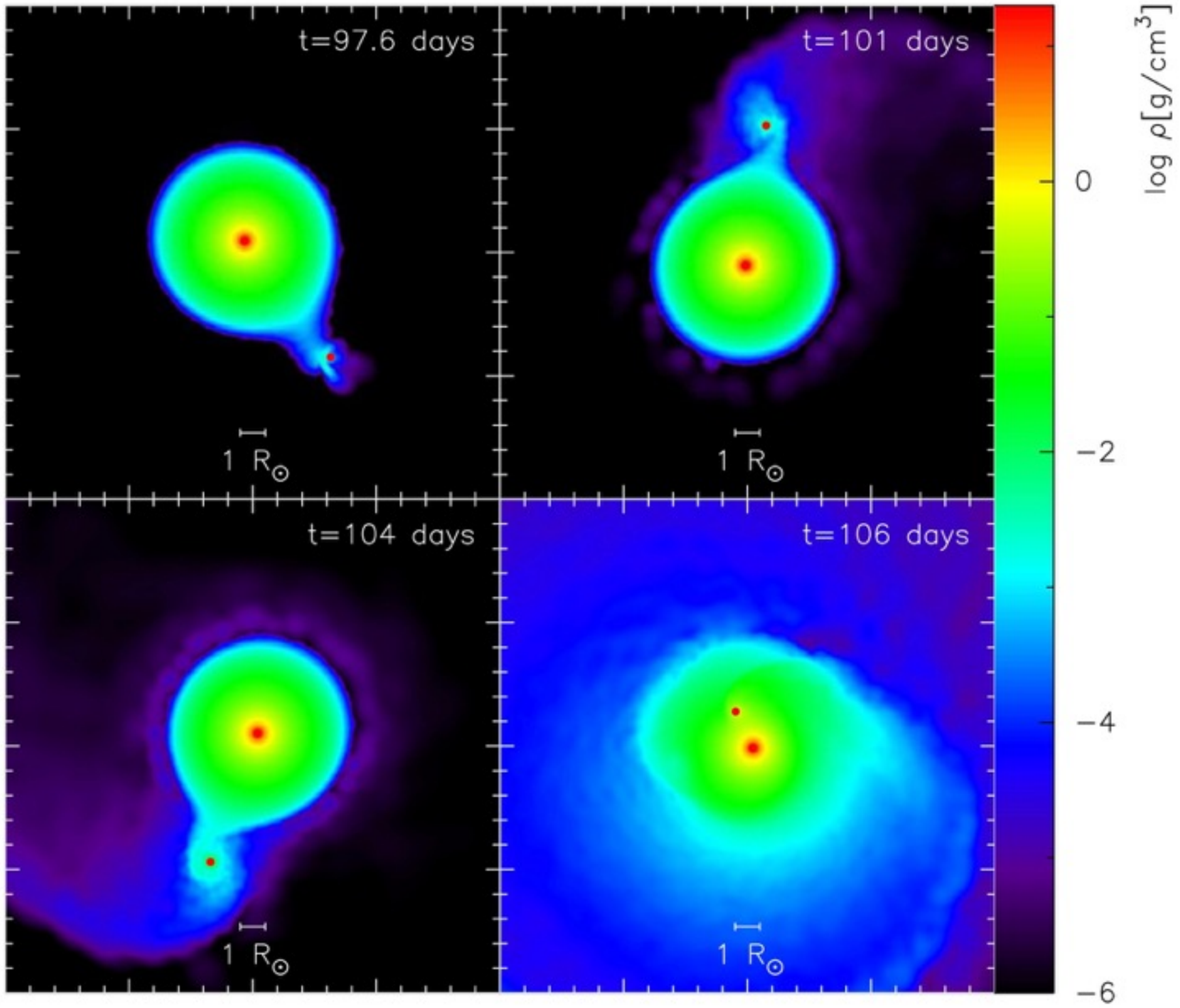

ROYAL ASTRONOMICAL SOCIETY

MNRAS **443,** 1319–1328 (2014) doi:10.1093/mnras/stu1226

Stellar mergers are common

C. S. Kochanek,[1,2★] Scott M. Adams[1,2] and Krzysztof Belczynski[3,4]

[1]*Department of Astronomy, The Ohio State University, 140 West 18th Avenue, Columbus, OH 43210, USA*
[2]*Center for Cosmology and AstroParticle Physics, The Ohio State University, 191 W. Woodruff Avenue, Columbus, OH 43210, USA*
[3]*Astronomical Observatory, Warsaw University, Al. Ujazdowskie 4, PL-00-478 Warsaw, Poland*
[4]*Center for Gravitational Wave Astronomy, University of Texas at Brownsville, Brownsville, TX 78520, USA*

Accepted 2014 June 11. Received 2014 June 11; in original form 2014 May 6

ABSTRACT

The observed Galactic rate of stellar mergers or the initiation of common envelope phases brighter than $M_V = -3$ ($M_I = -4$) is of the order of ∼0.5 (0.3) yr^{-1} with 90 per cent confidence statistical uncertainties of 0.24–1.1 (0.14–0.65) and factor of ∼2 systematic uncertainties. The (peak) luminosity function is roughly $\mathrm{d}N/\mathrm{d}L \propto L^{-1.4\pm0.3}$, so the rates for events more luminous than V1309 Sco ($M_V \simeq -7$ mag) or V838 Mon ($M_V \simeq -10$ mag) are lower at $r \sim 0.1$ and ∼0.03/year, respectively. The peak luminosity is a steep function of progenitor mass, $L \propto M^{2-3}$. This very roughly parallels the scaling of luminosity with mass on the main sequence, but the transients are ∼2000–4000 times more luminous at peak. Combining these, the mass function of the progenitors, $\mathrm{d}N/\mathrm{d}M \propto M^{-2.0\pm0.8}$, is consistent with the initial mass function, albeit with broad uncertainties. These observational results are also broadly consistent with the estimates of binary population synthesis models. While extragalactic variability surveys can better define the rates and properties of the high-luminosity events, systematic, moderate depth ($I \gtrsim 16$ mag) surveys of the Galactic plane are needed to characterize the low-luminosity events. The existing Galactic samples are only ∼20 per cent complete, and Galactic surveys are (at best!) reaching a typical magnitude limit of $\lesssim 13$ mag.

Key words: stars: individual: M85 OT2006-1 – stars: individual: M31 RV – stars: individual: V838 Mon – stars: individual: V1309 Sco – stars: individual: V4332 Sgr – stars: individual:

Table A1. Properties of merger candidates.

Object	Peak mag		Dist	$E(B-V)$	Peak abs mag		Progenitor		Mass
	V	I	(kpc Mpc^{-1})	(mag)	M_V	M_I	M_V	M_I	$M_\odot$
V4332 Sag	8.5	6.9	1.8	0.30	−3.7	−4.9	5.1	4.0	1
V838 Mon	7.0	5.5	6.1	0.80	−9.4	−9.8	−0.3	0.1	5 − 10
OGLE -BLG-360	16.5	11.3	8.2	2.00	−4.3	−6.7	−1.5	−1.9	1 − 2
V1309 Sco	8.0	7.0	3.0	0.80	−6.9	−6.7	2.1	1.2	1 − 3
M31 RV	17.0	15.5	1.0	0.30	−8.9	−10.0			–
M85 OT	19.7	18.5	17.8	0.20	−12.2	−13.1			<7

Note: The appendix provides a more detailed discussion, parameter ranges and references for each object. The distances are in kpc (Mpc) for the Galactic (extragalactic) objects. We have included the estimated circumstellar extinction for OGLE-2002-BLG-360 in the estimate of $E(B-V)$. Due to extinction and light-curve sampling, the peak V magnitude of this event is more uncertain that the other table entries.

SN 2009ip

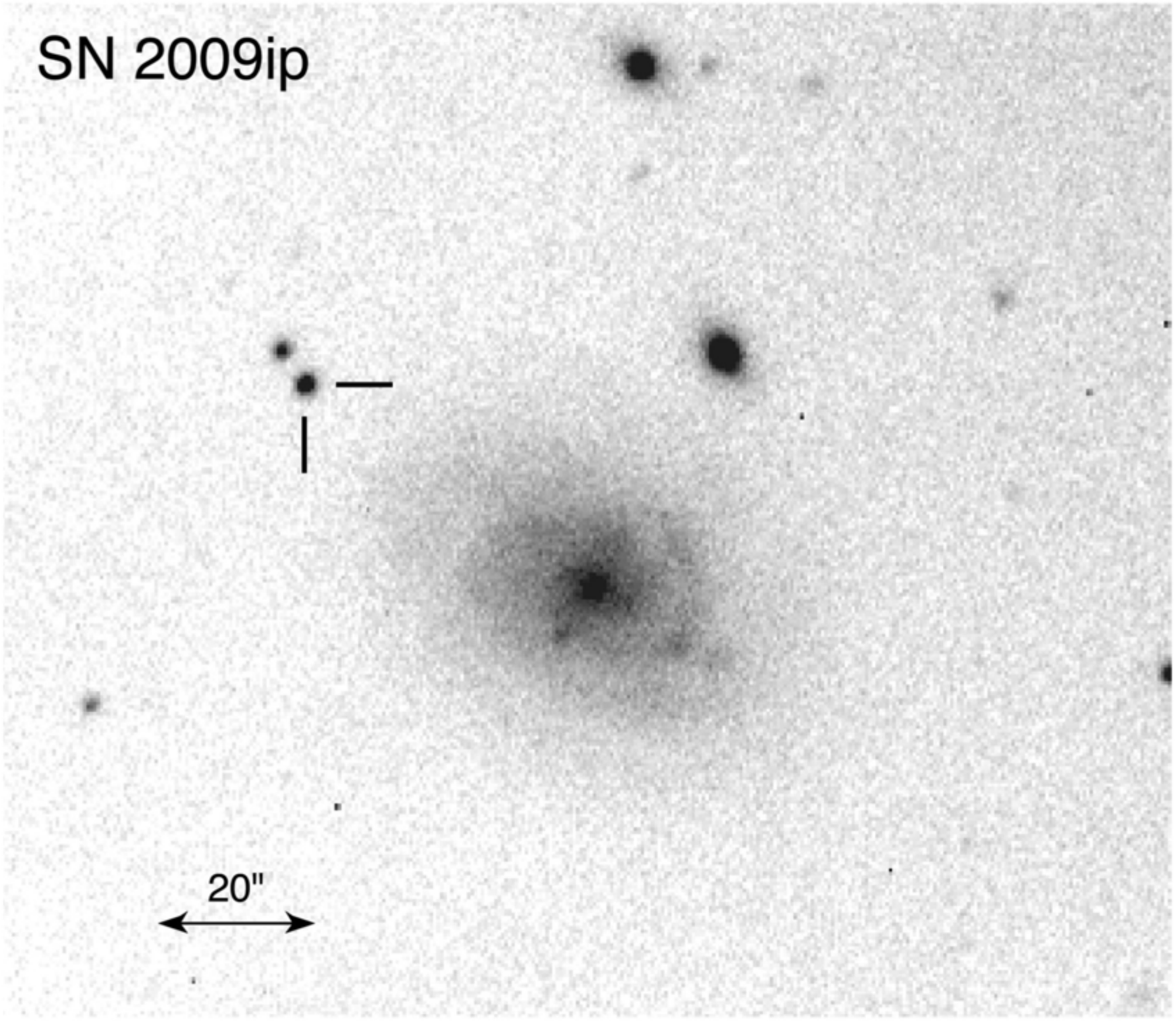
SN 2009ip
20"

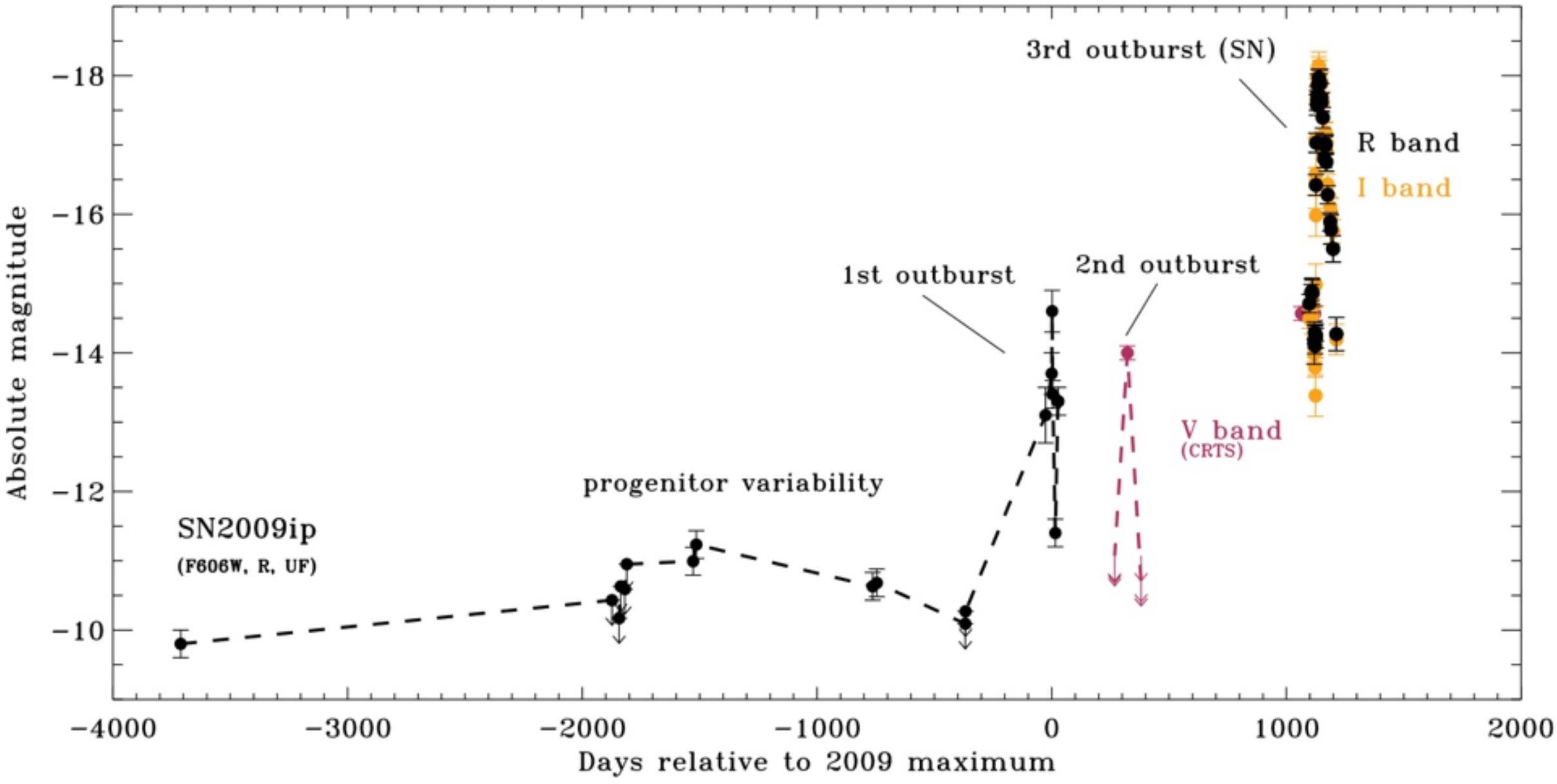
3rd outburst (SN)
R band
I band
1st outburst
2nd outburst
V band
(CRTS)
progenitor variability
SN2009ip
(F606W, R, UF)
Absolute magnitude
−18
−16
−14
−12
−10
−4000
−3000
−2000
−1000
0
1000
2000
Days relative to 2009 maximum

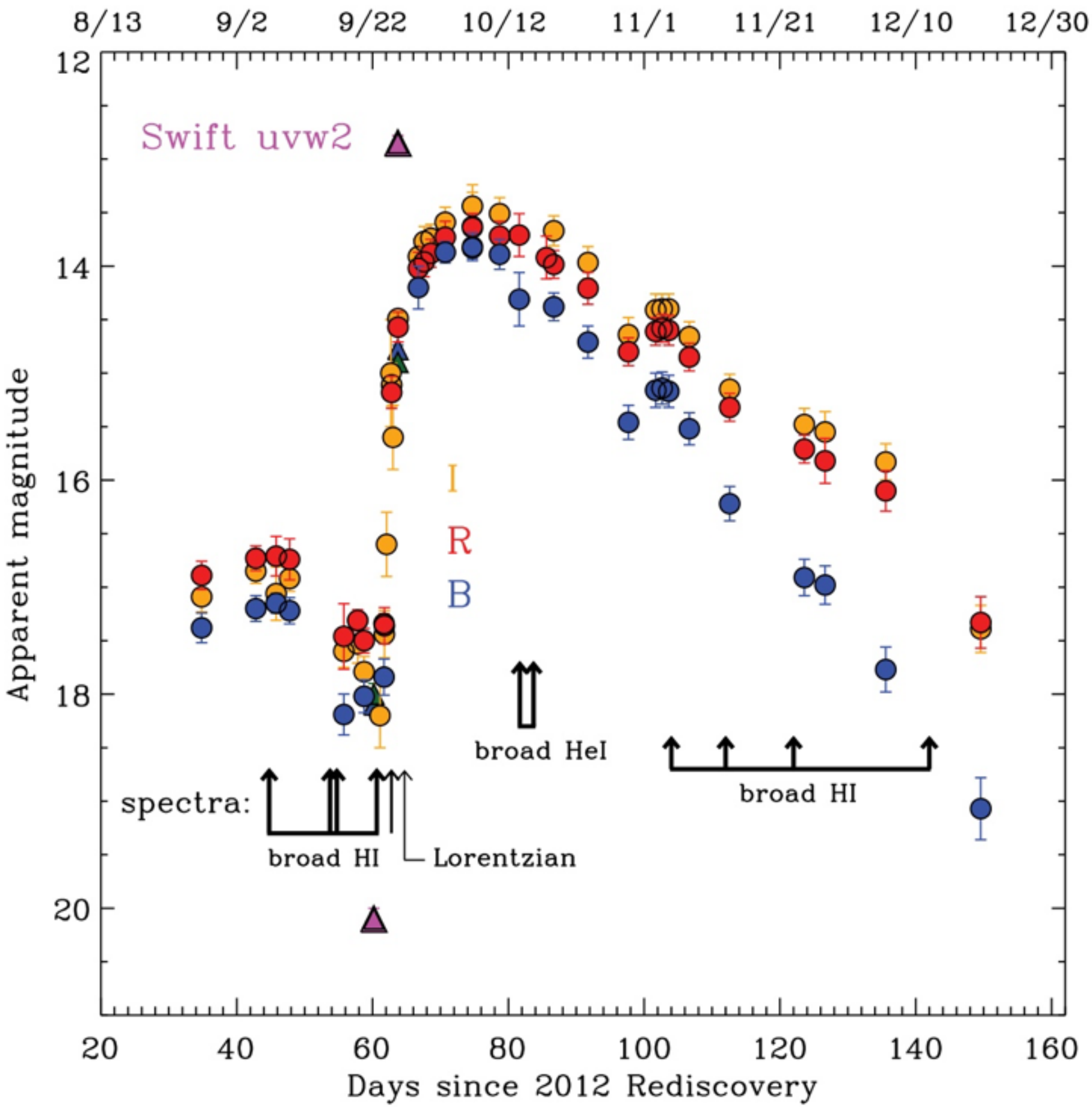
8/13
9/2
9/22
10/12
11/1
11/21
12/10
12/30
12
14
16
18
20
Apparent magnitude
Swift uvw2
I
R
B
broad HeI
broad HI
spectra:
broad HI
Lorentzian
20
40
60
80
100
120
140
160
Days since 2012 Rediscovery

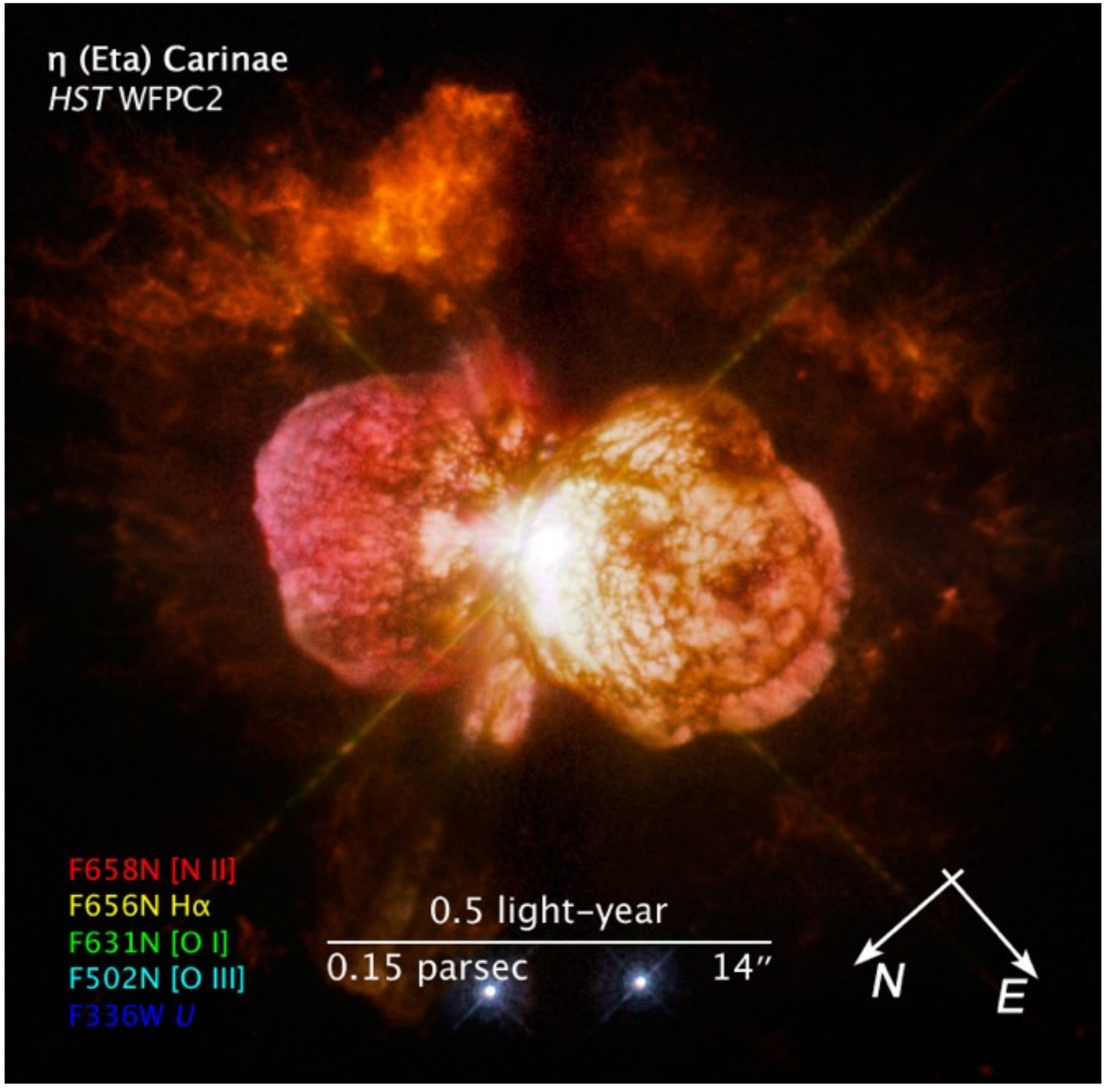
η (Eta) Carinae
HST WFPC2
F658N [N II]
F656N Hα
F631N [O I]
F502N [O III]
F336W *U*
0.5 light-year
0.15 parsec
14″
N
E

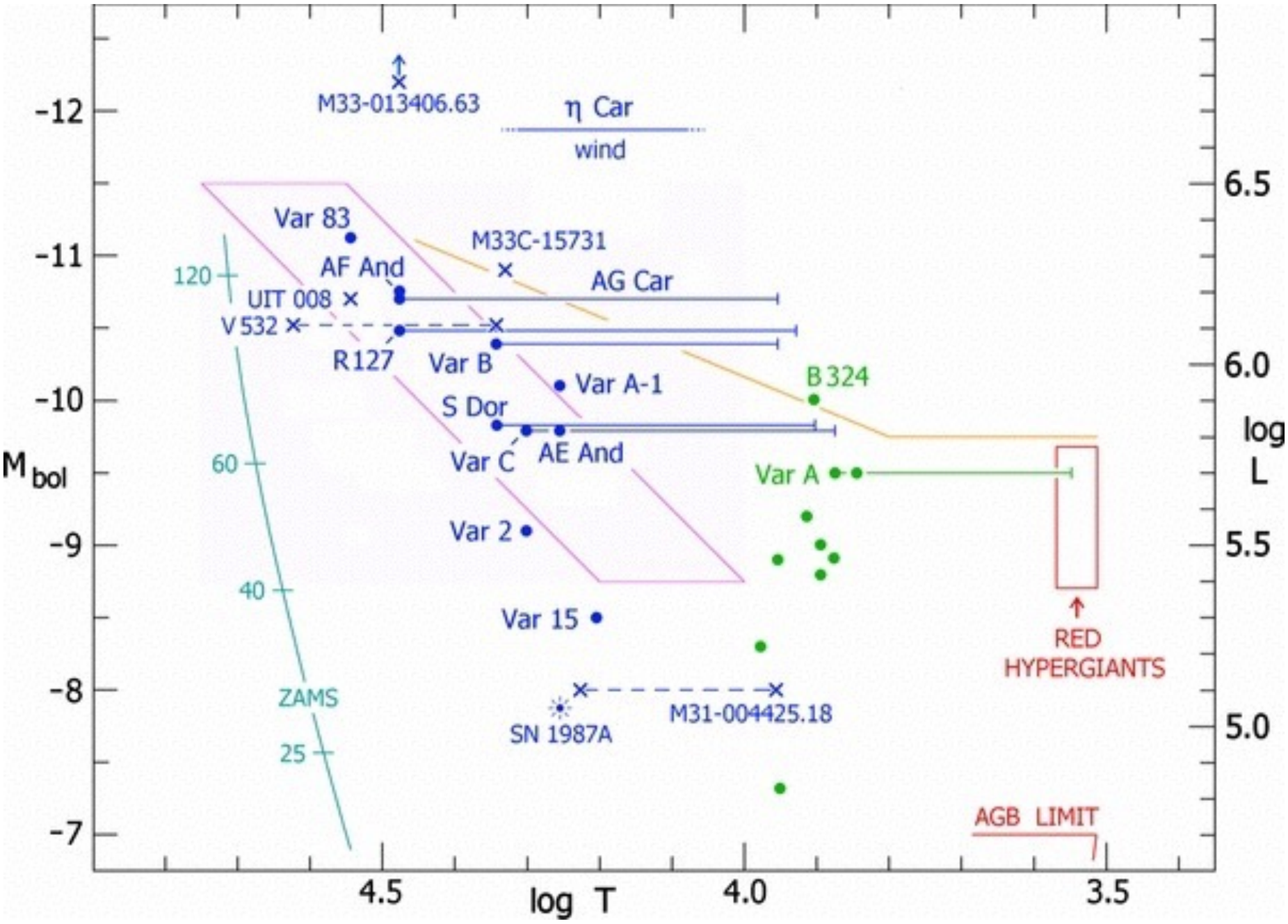
M33-013406.63
η Car
wind
Var 83
M33C-15731
AF And
AG Car
120
UIT 008
V 532
R127
Var B
Var A-1
B 324
S Dor
Var C
AE And
60
Var A
Var 2
40
Var 15
RED
HYPERGIANTS
ZAMS
25
SN 1987A
M31-004425.18
AGB LIMIT
-12
-11
-10
-9
-8
-7
M bol
6.5
6.0
5.5
5.0
log
L
4.5
log T
4.0
3.5